UNIVERSITY OF CRETE

DEPARTMENT OF MATERIAL SCIENCE AND TECHNOLOGY

Synthesis of carboxylated chitosan derivatives for tissue engineering applications

---

Bachelor thesis of

Vasileios Tsampallas

Supervisor:

Maria Vamvakaki

Heraklion Crete, October 2021

Table of Contents

Page

Abstract

Chitosan, a partially deacetylated derivative of a natural polysaccharide, chitin, is one of the most popular biomaterials, due its excellent biocompatibility, biodegradability and strong antimicrobial properties. However, it has limited solubility at pH values close to neutral pH, because of its very stable crystalline structure arising from strong inter- and intra-molecular hydrogen bonds. The conversion of chitosan into a water-soluble form can be achieved using different methods. One such modification approach, focuses on the addition of carboxymethyl groups onto either its amino (C_2-NH_2) or its hydroxyl (3-OH, 6-OH) groups or even onto both of these groups simultaneously.

In this bachelor thesis, a series of different carboxylated chitosan derivatives modified either through its amino, hydroxyl or both side-groups, with different degrees of modification were prepared. The synthesized samples of modified chitosan were characterized by Fourier-transform infrared (FTIR) and nuclear magnetic resonance (NMR) spectroscopies and thermogravimetric analysis (TGA). These materials will be employed to investigate the effect of the specific functionalization of the chitosan side-groups on its biological properties in tissue engineering applications.

Abbreviations

CS	Chitosan
CM	Carboxymethyl
CMC	Carboxymethyl chitosan
O-CMC	O-Carboxymethyl chitosan
N-CMC	N-Carboxymethyl chitosan
N,N-CMC	N-disubstituted Carboxymethyl chitosan
N,O-CMC	N,O-Carboxymethyl chitosan
DS	Degree of substitution
N-sub	N-substitution
DS-N	Degree of substitution of the amine groups
DS-O	Degree of substitution of the hydroxyl groups
GA	Glyoxylic acid
RT	Room Temperature
MCA	Monochloroacetic acid
SB	Sodium Borohydride
NaOH	Sodium hydroxide
BMP-2	Bone morphogenetic protein-2
^{1}H NMR	Proton nuclear magnetic resonance
^{13}C NMR	Carbon-13 nuclear magnetic resonance
HSQC	Heteronuclear Single Quantum Coherence
FT-IR	Fourier-transform infrared spectroscopy

TGA	Thermogravimetric analysis
ppm	Parts per million
Fmoc	Fluorenylmethoxycarbonyl protecting group
Boc	tert-Butyloxycarbonyl protecting group

Acknowledgements

First and foremost, I would like to express my deep and sincere gratitude to my research supervisor, Professor Maria Vamvakaki for giving me the opportunity to do my first research in polymer chemistry and guided me through the whole process. I would also like to thank Professor Maria Chatzinikolaidou who agreed to be a member of my committee. Also, my special thanks go to Dr. Maria Kaliva who guided me throughout the year, supporting me, giving me advices and evaluating my progress. She has taught me the methodology to carry out research and to present the research work as clearly as possible. It was a great privilege and honor to work and study under her guidance.

In addition, I would like to say thanks to my research colleagues of the Synthetic Materials Chemistry lab for the helping me in everything that I needed and for their support. I would also like to thank my friends who have supported me and cheered me up when I was down throughout the whole year.

Last but not least, I am extremely grateful to my parents Emmanouil and Anastasia for their love, caring and sacrifices for educating and preparing me for my future. I am very thankful to my twin brother Ioannis and my sister Stamatia for their love and continuing support. I would not have achieved anything without my family, thank you from my heart.

Chapter 1

1. Introduction

1.1 Tissue engineering

Tissue engineering can be defined as the growth of a new tissue using living cells guided by the structure of a substrate made of a natural or synthetic material. This substrate is called a scaffold. The scaffold materials are important since they must be compatible with the cells and guide their growth. Most scaffold materials are biodegradable or resorb as the cells grow. Scaffolds are more often made from natural or synthetic polymers, but for hard tissues, such as bone and teeth, inorganic ceramic compounds, i.e. calcium phosphates, can be also utilized. The tissue is grown in vitro and implanted in vivo.[1]

Tissue engineering involves the design of scaffolds for the modulation of cellular growth and differentiation. The scaffolds utilized for tissue engineering require certain biological and mechanical properties, similar to the natural extracellular matrix (ECM), for their functioning. Some important features for the production of scaffolds for tissue engineering are[2]:

- The presence of interconnecting pores of appropriate dimensions to promote tissue integration and vascularization
- Controlled biodegradability and bioresorbability to match the regenerated tissue growth
- Presence of favourable surface functionalities to promote cell attachment, differentiation and proliferation
- Optimal mechanical properties which are similar to the intended site of implantation
- Low to negligible toxicity and,
- Easy fabrication procedures to achieve desirable shapes and sizes

1.2 Biomaterials

Biomaterials is a wide-ranging field, encompassing aspects of basic biology, medicine, engineering and materials science.[3] **Biomaterial** is defined as any

material that is intended to interface with biological systems to evaluate, treat, augment, or replace any tissue, organ or function of the body.[4] Biomaterial science includes subjects related to materials science, such as the mechanical properties of materials or the surface modification of implants, as well as biological topics such as immunology, toxicology, and wound healing processes. [3]

Because the ultimate goal of biomaterials use is to improve human health by restoring the function of natural living tissues and organs in the body, it is essential to understand the relationships between the structure, properties and functions of biological materials.[1] One of the most important concepts in biomaterials science is that of biocompatibility.[3] **Biocompatibility** is the ability of a material to perform with an appropriate host response in a specific application.[4]

1.3 Types of Biomaterials

Materials are classified as organic if they contain carbon atoms or inorganic if they do not.[3] More specifically, biomaterials are divided into three categories:

- Metals
- Ceramics and
- Polymers

1.4 Naturally Derived and Synthetic Polymers

Polymers are organic materials comprising long chains that are held together by covalent bonds. Polymers are widely used in biomedical applications because of their favorable physical and chemical properties.[5] There are two main categories of polymers: **naturally derived** and **synthetic polymers**.

Natural polymers can be derived from sources within the human body such as collagen and hyaluronic acid or from nature such as chitosan and alginate. One of the most common natural biomaterials is the protein collagen. In addition to proteins, natural polymers can be derived from sugars (carbohydrates). One important example of a carbohydrate polymer found in human tissues is hyaluronic acid. On the other hand, **chitosan** and alginate are other carbohydrate-derived materials, that are non-human, and can be found in arthropod exoskeletons and seaweed, respectively.[3]

There are several polymer sub-classes that are useful biomaterials, in that each may be particularly suited for a certain tissue type. Two important examples are elastomers and hydrogels. Elastomers can sustain substantial deformation at low stresses and return rapidly to their initial dimensions upon release of the stress. These materials can be suitable for cardiovascular applications, where elasticity is an important property. On the other hand, hydrogels exhibit the ability to swell in water and to retain a significant amount of water within their structures without completely dissolving. Hydrogels have been explored for a variety of soft tissue applications.[3,4]

1.5 Chitosan: structure and properties

Chitin is one of the most abundant polysaccharides on earth, present in the exoskeleton of crustaceans, insects and fungal cell walls (**Fig. 1.1**). It is a naturally occurring mucopolysaccharide and ranks second after cellulose in terms of abundance. Chitin consists of a sugar backbone with β-1,4-linked glucosamine units, and is a derivative of cellulose, with the hydroxyl groups being replaced by amine groups that possess a high degree of acetylation.[6,7]

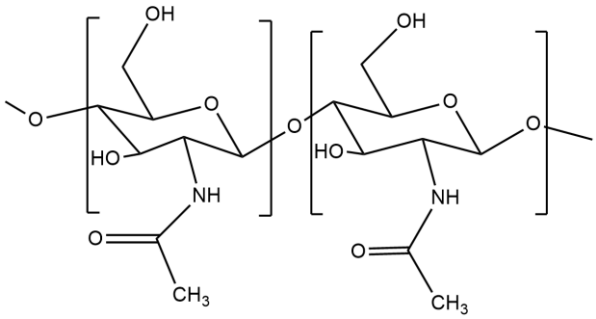

Fig. 1.1 *The structure of chitin*

The main derivative of chitin is chitosan, a cationic copolymer of glucosamine and N-acetylglucosamine, produced by the alkaline deacetylation of chitin (**Fig. 1.2**).[7,8] Chitosan (CS) has a unique set of useful characteristics such as biocompatibility, biodegradability, biorenewability, bioadhesivity and nontoxicity. These important properties render it particularly attractive in the biomedical field.[8] Chitosan and its derivatives have numerous application in pharmaceutics, biomedicine[9–11], water treatment[12,13], cosmetics[14], agriculture[15] and the food industry[16]. Moreover,

chitosan itself has been reported to have various beneficial pharmacological properties for drug delivery and tissue engineering applications.[6]

Owing to its negligible toxicity and biodegradability, chitosan has found considerable application in the field of tissue engineering namely[6]:

- Skin tissue engineering
- Bone tissue engineering
- Cartilage tissue engineering
- Neural tissue engineering and
- Vascular tissue engineering

However, the applications of chitosan suffers severe limitations since it is insoluble in neutral or alkaline pH and in common organic solvents, because of its highly crystalline structure arising from strong inter- and intra-molecular hydrogen bonds. Chitosan is soluble only in acidic aqueous solutions below pH 6.5 (below the pK_a of chitosan).[8]

Chitosan has three reactive groups in its units[17]:

- A primary hydroxyl group (*6-OH)*
- A secondary hydroxyl group and *(3-OH)*
- An amino group *(C_2-NH_2)*

The conversion of chitosan into a water-soluble form can be achieved by different methods. One such modification approach, focuses on the addition of carboxymethyl groups onto either its amino (C_2-NH_2) or its hydroxyl (3-OH, 6-OH) groups or even onto both of these groups, simultaneously.

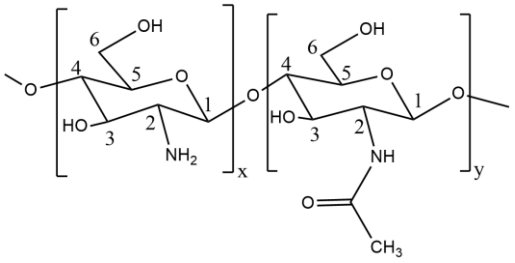

Fig.1.2. *Chemical structure of chitosan*

1.6 Carboxymethyl chitosan derivatives

There are four kinds of derivatives of carboxymethyl chitosan (CMC) which are: N,N dicarboxymethyl chitosan (N,N-CMC), N-carboxymethyl chitosan (N-CMC), O-carboxymethyl chitosan (O-CMC) and N,O-carboxymethyl chitosan (N,O-CMC). The name depends on the group onto which the carboxymethyl group is attached. There are two main methods disclosed in the literature for the preparation of N,O-carboxymethyl chitosan derivatives (**Fig.1.3**).[8]

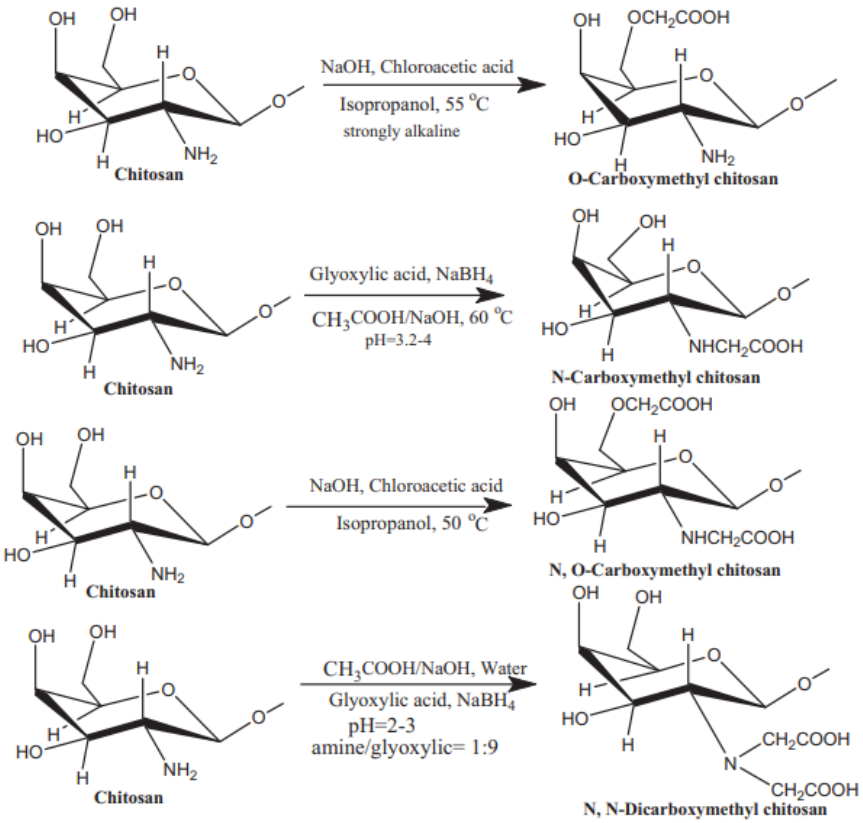

Fig.1.3. *Carboxymethylation of chitosan: An overview of the different type of reactions used for the modification of chitosan.* [18]

1.7 Synthesis of carboxymethyl chitosan

1.7.1 Reductive alkylation

The first approach for the synthesis of either N-carboxymethyl chitosan (N-CMC) or N,N-dicarboxymethyl chitosan is by reductive alkylation. More specifically, the NH_2

group of the chitosan unit is reacted with the aldehyde group of glyoxylic acid, followed by a hydrogenation reaction with $NaBH_4$ or $NaCNBH_3$ to give N-carboxymethyl chitosan. With this method, the carboxymethyl substituent is placed exclusively on the N-atom, in the absence of O-substitution. However, the reactivity of the aldehyde group is so high, that along with N-carboxymethyl chitosan, partially di-substituted N-carboxymethyl chitosan (N,N-CMC) is unavoidably produced, even under mild conditions; therefore, the term N-carboxymethyl chitosan implies that a substantial fraction is di-substituted. One important factor in this method is the ratio of amine (chitosan) groups to glyoxylic acid used as well as the reaction conditions.[8]

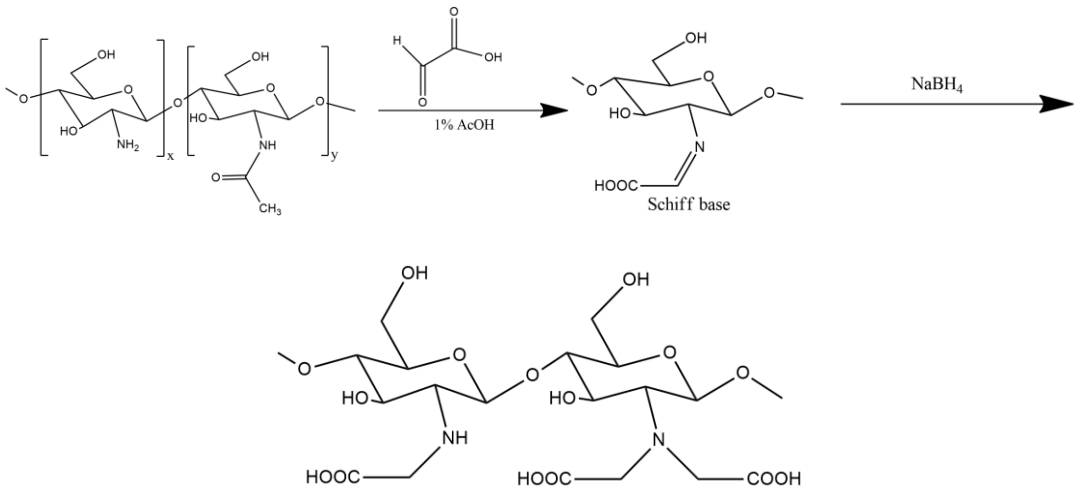

Fig.1.4. *Reductive alkylation of chitosan: N-CMC and N.N-CMC*

1.7.2 Direct alkylation

The second approach for the synthesis of CMC involves the direct alkylation using monochloroacetic acid at different pH values. The direct alkylation method utilizes monohalocarboxylic acids, such as monochloroacetic acid, to prepare N-carboxyalkyl and O-carboxyalkyl chitosan derivatives at different reaction conditions .According to the literature, by choosing the proper reaction conditions the carboxyalkylation of chitosan can be directed toward the amine rather than the hydroxyl groups. Usually, the carboxymethylation of chitosan takes place in a mixture of water/isopropyl alcohol. When carboxymethylation of chitosan with monochloroacetic acid takes place in mildly alkaline media at pH 8–8.5, only the amine groups are activated thus

only N-substitution takes place. On the other hand, at higher pH values, the hydroxyl groups are activated and therefore the reaction is favored. However the reactivity of the amine groups is so high that along with O-carboxymethyl chitosan (O-CMC), N-carboxymethyl chitosan (N-CMC) is unavoidably produced, even under mild conditions.[8]

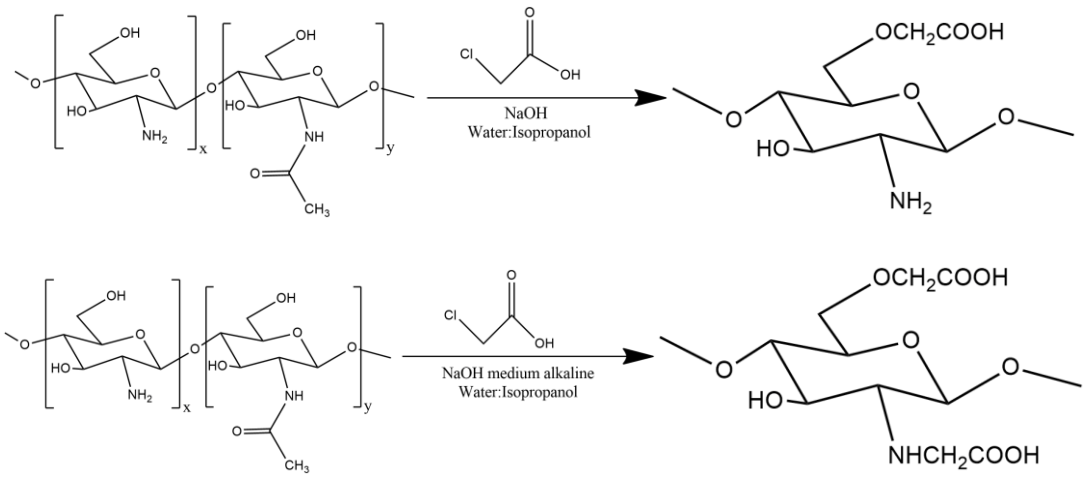

Fig.1.5. *Direct alkylation of chitosan using monochloroacetic acid. Synthesis of O-CMC (a) and N,O-CMC (b)*

1.8 Biomedical and pharmaceutical applications of carboxymethyl chitosan

Carboxymethyl chitosan derivatives find numerous application in the biomedical field, such as in wound healing, tissue engineering, drug/enzyme delivery, bioimaging and cosmetics, because of its favorable biological properties including antimicrobial, anticancer, antitumor, antioxidant and antifungal activities.(**Fig 1.4.**)[19]

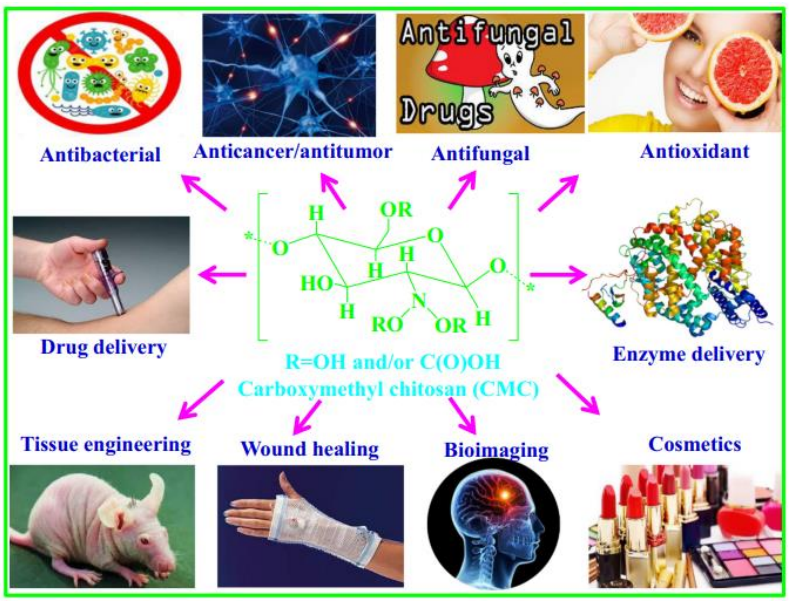

Fig.1.6. *Applications of the carboxymethyl chitosan (CMC) derivatives*[19]

Carboxymethyl chitosan derivatives are valuable materials as scaffolds because they can be degraded when new tissue is formed with minimum toxic degradation products and inflammatory reactions. One important example is the N,N-CMC to deliver bone morphogenetic protein in order to repair the articular cartilage.[20] Another significant research showed that O-CMC-BMP-2 modified titanium substrates decrease bacterial adhesion and improve cell function. Moreover, this substrate proved the high capacity of O-CMC to enhance the tissue integration as well as implant durability.[21] Likewise, injectable O-CMC/gelatin/nanohydroxyapatite gels were utilized for the treatment of irregular small bone defects (with minimum clinical invasion) and for bone cell delivery in mice, and it was exhibited that the stability of the in situ formed gels was dependent to the crosslinking degree and the amount of O-CMC.[22]

1.9 Current work

Even though, there are a variety of different studies employing the above methods to synthesize CMC, it is not yet clear how to direct the carboxylation to the amine or hydroxyl groups of chitosan alone, how to regulate the DS, and how their modified nature can be capitalized in order to produce even more potent biomaterials. Therefore, in this work, the carboxymethylation of chitosan using glyoxylic acid and

monochloroacetic acid at different reaction conditions was investigated. A series of different carboxylated chitosan derivatives, modified either through its amino, hydroxyl or both side-groups, with different degrees of modification were prepared. The synthesized samples were characterized by Fourier-transform infrared (FTIR) and nuclear magnetic resonance (NMR) spectroscopies and thermogravimetric analysis (TGA). These materials will be employed to investigate the effect of the specific functionalization of the chitosan side-groups on its biological properties in tissue engineering applications.

Chapter 2

2 Materials and Methods

2.1 Materials

Chitosan (10 cps), with degree of deacetylation 90% and with an average molecular weight (30.000 g/mol) was purchased from Glentham Life Sciences. Chloroacetic acid ≥ 99.0%, glyoxylic acid solution 50 wt. % in H_2O, and sodium borohydride (ReagentPlus 99%) were purchased by Sigma-Aldrich. In addition, sodium hydroxide pellets ≥ 98.0% was purchased from AppliChem Panreac ITW Companies. Acetone ≥99.5% was purchased from Honeywell. Moreover, propan-2-ol (isopropanol) ≥99.9% was purchased from Carlo Erba. Finally, deuterium oxide ≥99.9% and deuterium chloride 35 wt. % solution in D_2O (99 atom % D) were purchased from Sigma-Aldrich. Milli-Q water with a resistivity of 18.2 MΩ*cm at 298K was obtained from a Milipore apparatus and was used in all experiments.

2.2 Synthesis of N-Carboxymethyl chitosan

N-carboxymethyl chitosan was synthesized as described previously by Muzzareli et al[23]. First chitosan powder (90% deacetylated) was suspended in ultrapure water. Then, glacial acetic acid (1% w/w) was added, to promote the dissolution of chitosan, at room temperature after stirring for 20 min. Next, glyoxylic acid (GA) (50% v/v solution) was introduced in the reaction solution. The molar ratio of glyoxylic acid/glucosamine units was altered from 1:1 to 4:1 (Table 2.1). After the addition of glyoxylic acid to the solution, the pH was adjusted to the desired value with sodium hydroxide (NaOH). All the reactions were allowed to proceed at room temperature. After the desired reaction time, sodium borohydride ($NaBH_4$) was added in the reaction vessel to hydrogenate the Schiff base double bond and the solution was left under stirring for another 30 mins. The modified CMCs were then isolate by precipitation in acetone at least 3 times, followed by centrifugation at 11.000 rpm. In addition, to protonate the Na salt of CM-chitosan derivatives, the polymers were diluted in ultrapure water and hydrochloric acid (1M) was added to adjust the pH at 2 and was stirred for 30 min. Then, CMC was precipitated in acetone, centrifuged at

11.000 rpm and dried under vacuum for 2 h. Finally, it was dissolved in ultrapure water and was lyophilized.

The N-Carboxymethyl chitosan derivatives synthesized under different reaction conditions are presented in **Table 2.1**.

Table 2.1. N-Carboxymethyl Chitosan Under Different Conditions

Sample	GA:$NaBH_4$ Molar ratio	GA:$NaBH_4$ Molar ratio	Reaction Time	pH
N1-1:1	Equimolar	1:3	1.5 h	4.5
N-1:1	Equimolar	1:3	Overnight	4
N2-2:1	2:1	1:3	Overnight	4
N-2:1	2:1 added in two portions	1:3	Overnight	4
N-3:1	3:1	1:3	Overnight	4
N3-3:1	3:1 added in three portions	1:3	Overnight	4
N-4:1	4:1	1:3	Overnight	4

2.3 Synthesis of Carboxymethyl chitosan using monochloroacetic acid

N,O-Carboxymethyl chitosan derivatives were synthesized via direct alkylation as described before[24–26]. More specifically, chitosan powder (90% deacetylated) and aqueous sodium hydroxide solution of different concentrations were added into a flask to swell at a given temperature overnight. Monochloroacetic acid (MCA), dissolved in isopropanol, was then added into the reaction mixture in equal portions and was allowed to react at the given temperature. The mixture was precipitated in acetone, centrifuged at 11.000 rpm and vacuum dried at room temperature. The products were CM-chitosan Na salt. To protonate the CM-chitosan Na salt derivatives, the polymers were diluted in ultrapure water and hydrochloric acid (1M) was added, to adjust the pH at 2, and the mixture was stirred for 30 min. Finally, the products were lyophilized.

The **N,O-10%** sample was synthesized following a slightly different procedure. More specifically, chitosan was suspended in isopropanol for 30 mins. Then, an aqueous NaOH solution, divided into five equal portions, was added to the stirred

slurry over a period of 25 mins and was stirred for an additional 30 mins. Subsequently, solid MCA was added in five equal portions at 1 min intervals. The reaction mixture was heated to 60°C and was stirred at this temperature for 3 h.

The CMC-derivatives synthesized and the reaction conditions are presented in **Table 2.2**.

Table 2.2. N,O-Carboxymethyl Chitosan Under Different Conditions

Sample	MCA-chitosan Molar ratio	Water:Isopropanol v/v	NaOH w/v%	Reaction Temperature (°C)	Reaction Time	pH
N,O-10%	8:1	1:4	**10**	60	3	8-8.5
N,O-12,5%	8:1	1:4	**12.5**	20	4	12
N,O-1-33%	8:1	1:1	**33**	20	4	14
N,O-2-33%	8:1	1:1	**33**	60	4	14
N,O-1-50%	8:1	1:1	**50**	20	4	14
N,O-2-50% 1h swelling	4:1	1:1	**50**	20	4	14
N,O-3-50% 24h swelling	4:1	1:1	**50**	20	4	14

2.4 ^{1}H -^{13}C NMR spectroscopy

Nuclear magnetic resonance (NMR) was used to confirm the formation of carboxymethyl chitosan derivatives (CMCs) and to determine the degree of carboxymethylation. More specifically, 30mg of each sample was dissolved in D_2O and placed in an NMR tube. The ^{1}H-NMR spectrum of CMCs was acquired at 353K or at 325K, using 500 MHz spectrometer (Avance Bruker). The ^{13}C-NMR and 2D spectrum of CMCs was acquired at 303K, using 500 MHz spectrometer (Avance Bruker). Carboxymethyl chitosan derivatives were dissolved in D_2O while chitosan was dissolved in D_2O/DCl.

2.5 FTIR spectroscopy

The synthesis of the carboxymethyl chitosan derivatives (CMCs) were confirmed by FTIR spectroscopy. FTIR spectra of chitosan and the CMCs were recorded on an Thermo and Scientific Nicolet 6700 FTIR spectrometer. The scanning range was 4000-400 cm^{-1} at a resolution of 4.

2.6 Thermogravimetric Analysis (TGA)

The thermal stability of the samples was determined by TGA measurements using a Perkin Elmer TG/DTA apparatus. The weight of sample used for each measurement was approximately 10mg. All measurements were carried out under a nitrogen atmosphere, by heating the material from room temperature to 550 ℃ at a heating rate of 10℃·min^{-1}.

Chapter 3

3.1 Results and Discussion

In this thesis, a series of carboxymethylated chitosan derivatives were synthesized by reductive alkylation or the direct alkylation method. In the first approach, the effect of the reaction time, the pH of the reaction solution and the molar ratio of glyoxylic acid/glucosamine units on the degree of substitution was investigated. More specifically, CMC samples were prepared at a molar ratio of glyoxylic acid/glucosamine units of 1:1, 2:1, 3:1 and 4:1, and reaction times between 1.5h to 24h. The pH value ranged from 4 to 4.5 (**Table 2.1**).

In the second method, we investigated how the degree of substitution is affected by the reaction time, the pH of the reaction solution, the NaOH concentration, the v/v ratio of water/isopropanol and the molar ratio of monochloroacetic acid/chitosan repeat units. In particular, a series of CMC samples were prepared, in which the molar ratio of monochloroacetic/chitosan sugar residues was varied between 4:1 and 8:1, the v/v ratio of the water/isopropanol mixture from 1:1 to 1:4, the NaOH concentration at 10%, 12%, 33% and 50%. Moreover, the reaction temperature was varied between 20°C and 60°C and the reaction time between 3 and 4 h (**Table 2.2**).

3.2 Characterization of chitosan

The chemical structure and the degree of deacetylation of chitosan were determined by ^{1}H NMR spectroscopy. **Figure 3.1** shows the ^{1}H NMR spectrum of chitosan at 353 K (80°C). The peak **1** at **4.9** ppm and **1'** at **4.6** ppm in the ^{1}H NMR spectrum of chitosan are assigned to the **H-1D** and **H-1A** protons, respectively (where D refers to the protons located at the deacetylated unit and A are the protons at the acetylated unit). The peak **d** at **2** ppm corresponds to the acetyl-protons, the peak **2** at **3.2** ppm is assigned to **H-1D**. In the region between **3.6** and **4** ppm are the protons **2', 3, 4, 5, 6** and **6'** are observed[28,29]. From the ratio of the integrals of the peaks corresponding to the d and 2 protons of chitosan, the degree of deacetylation was found approximately 90%.

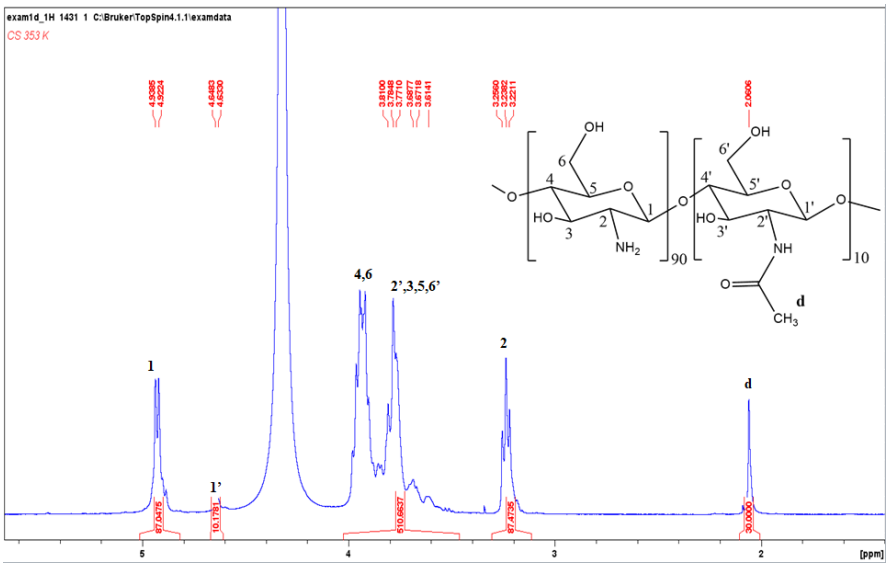

Fig.3.1. *^{1}H NMR spectrum of chitosan in D_2O/DCl at 353 K*

Moreover, the chemical structure of chitosan was studied by ^{13}C NMR spectroscopy. **Figure 3.2** shows the ^{13}C NMR spectrum of chitosan at 301K (28 ℃). The assignment of the carbons of chitosan is as following: peak **d** is the carbon of the methyl group (25 ppm), peak **C2** is the 2-carbon of deacetylated residue (59 ppm), peak **C6** is the 6-carbon of deacetylated residue(63 ppm), peak **C3** is the 3-carbon of the deacetylated residue (73 ppm), peak **C5** is the 5-carbon of the deacetylated residue (78 ppm), peak **C4** is the 4-carbon of deacetylated residue (79 ppm), peak **C1** is the 1-carbon of deacetylated residue (100 ppm) and **a** is the carbon at the acetyl group (178 ppm).[30]

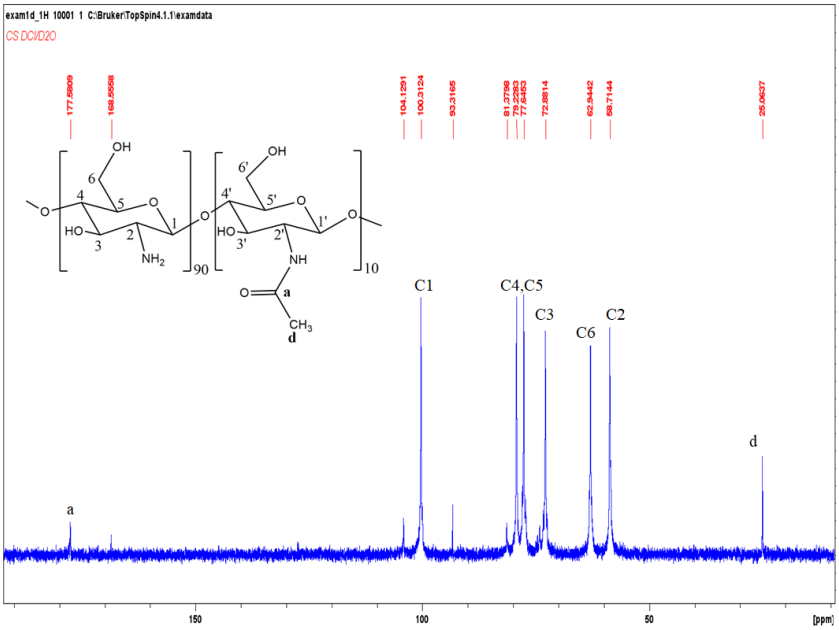

Fig.3.2. *^{13}C NMR spectrum of chitosan in D_2O/DCl at 301 K*

Finally, 2D HSQC (Heteronuclear Single Quantum Coherence) NMR spectroscopy was used for the characterization of the chemical structure of chitosan. **Figure 3.3** shows the HSQC NMR spectrum of chitosan at 301 K (28 °C). The 2D NMR spectrum confirms the corresponding peaks from the proton and carbon NMR. In particular, the ^{1}H-^{13}C correlation for **H1**/**C1** are observed at 4.9/100, those for **H3-H5**/**C3-C5** appeared at 3.6-4.0 ppm/73-81 ppm and the three methyl hydrogen atoms **Hd**/**CH_3** appear at 2.0 ppm/25 ppm. The carbon **C2** signal at 59 ppm shows two hydrogen correlations at 3.2 ppm (H2) and 3.9 ppm (H2') in the HSQC NMR spectrum. The carbon **C6** signal at 63 ppm shows also two hydrogen correlations at 3.7 ppm (H6') and 3.9 ppm (H6) on the HSQC NMR spectrum.

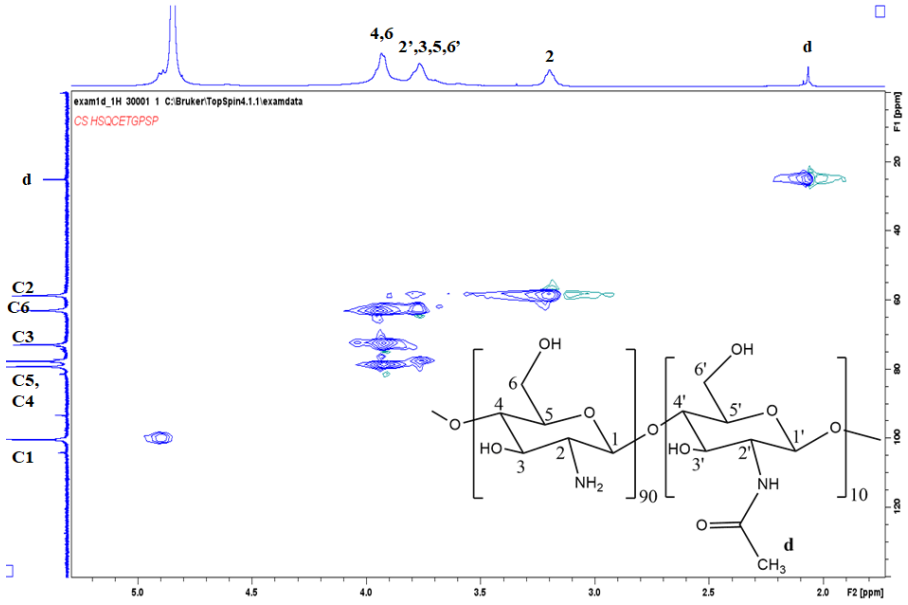

Fig.3.3. *HSQC NMR spetrum of chitosan in D_2O/DCl at 301 K*

Moreover, the chemical structure of chitosan was examined by FTIR spectroscopy. **Figure 3.4** shows the FTIR spectra of chitosan. The characteristic peaks of chitosan appear at 3455 cm^{-1} (**O-H stretching**), 2923-2867 cm^{-1} (**C-H stretching**), 1645 cm^{-1} (**C=O stretching**), 1598-1600 cm^{-1} (**N-H bending**), 1154 cm^{-1} (**bridge-O stretching**) and 1030 cm^{-1} (**C-O stretching**) of the primary hydroxyl group.[31,32]

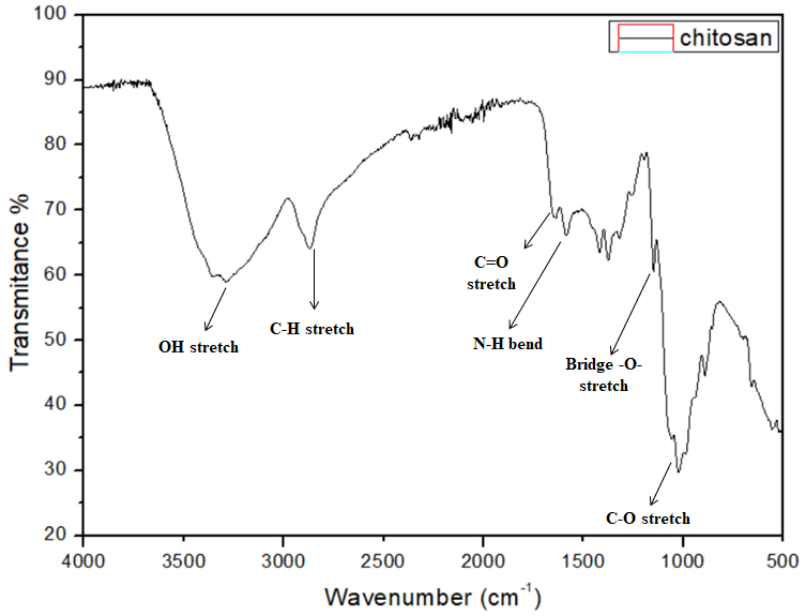

Fig.3.4. *FT-IR spectrum of chitosan*

Furthermore, the thermal properties of chitosan were investigated. **Figure 3.5** shows the TGA curve of chitosan, which shows one degradation progress, occurring in the range of 250-400 ℃ with a weight loss of 60 % assigned to the disintegration of chitosan via deacetylation and the cleavage of the glycosidic linkages. At temperatures above 320 ℃, a continuous decrease in the sample weight was observed up to 500 ℃, at which ~34% of the material remained as residue[33–35]

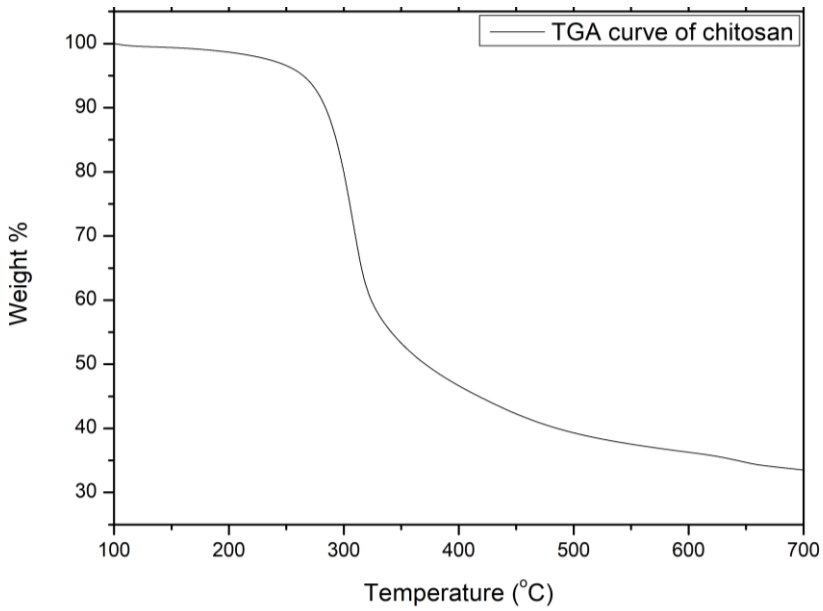

Fig.3.5. *TGA curve of chitosan*

3.3 Characterization of N-carboxymethyl chitosan derivatives

The successful synthesis of N-carboxymethyl chitosan derivatives was verified by ^{1}H NMR spectroscopy. **Figure 3.6** shows the ^{1}H NMR spectra of a N-carboxymethyl chitosan derivative prepared with 1:1 molar ratio of glyoxylic acid/glucosamine in comparison to the spectrum of chitosan at 353K.

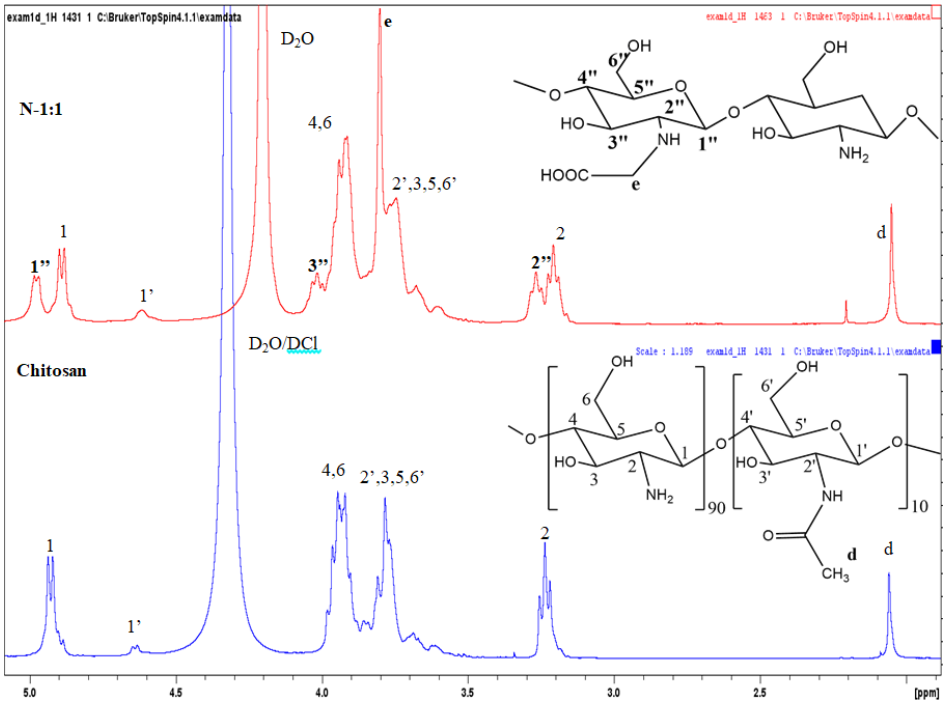

Fig.3.6. *^{1}H NMR spectra of chitosan and N-1:1 at 353 K*

The ^{1}H-NMR spectrum of N-CMC, N1-1:1 shows four new peaks at **3.27**, **3.8, 4.1** and **4.95** ppm (**Figure 3.6**). The peak **2"** at **3.27** ppm, the peak **e** at **3.8** ppm, the peak **3"** at **4.1** ppm and the peak **1" at 4.95 ppm** in the ^{1}H NMR spectrum were assigned to the **H-2D**, **N-CH$_2$COOH**, **H-3D** and **H-1D** protons of the modified structural unit, respectively. The degree of substitution was determined from the ^{1}H NMR spectra by rationing the integrals of the peaks **1"**to **1**. The degrees of substitution of all the N-carboxymethyl chitosan derivatives prepared in this study are presented at **Table 3.1**. The degree of substitution (DS) is defined as the number of modified groups per 100 structural units of the chitosan. In addition, the term N-substitution (N-sub) refers to the degree substitution of the 90 deacetylated structural units.

Table 3.1 Degree of substitution of N-carboxymethyl chitosan derivatives					
Samples	**Glyoxylic:glucosamine Molar Ratio**	**Time (h)**	**pH**	**DS (%)**	**N-sub (%)**
N1-1:1	1:1	1.5h	4.5	**31%**	**34%**
N-1:1	1:1	24h	4	**40%**	**44%**
N2-2:1	2:1 **added in two portions**	24h	4	**58%**	**64%**
N-2:1	2:1	24h	4	**50%**	**50%**
N-3:1	3:1	24h	4	**63%**	**70%**
N3-3:1	3:1 **added in three portions**	24h	4	**64%**	**71%**
N-4:1	4:1	24h	4	**66%**	**73%**

Figure 3.7 shows the ^{1}H NMR spectra of N-carboxymethyl chitosan derivatives, prepared with different mole ratios of glyoxylic acid/glucosamine for the same reaction time, at 353 K in comparison to the spectrum of chitosan.

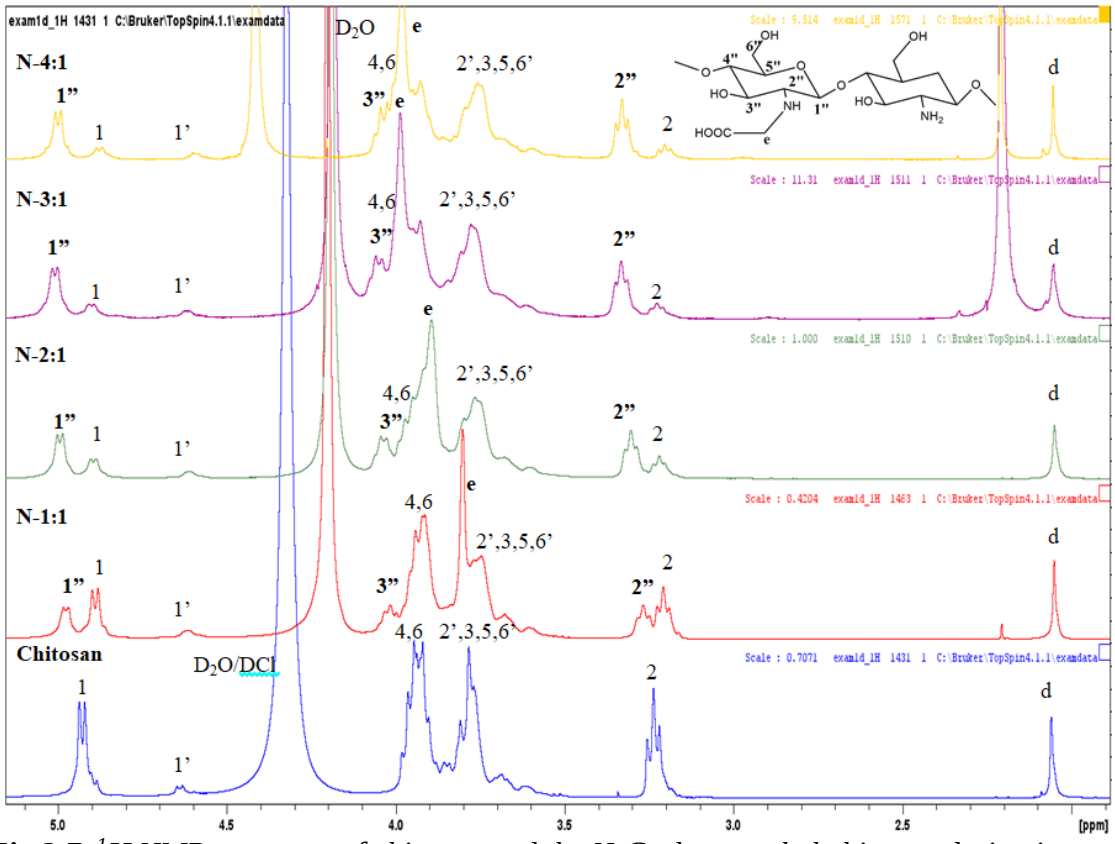

Fig.3.7. *^{1}H NMR spectrum of chitosan and the N-Carboxymethyl chitosan derivatives, prepared with different mole ratios of glyoxylic:glucosamine units for the same reaction time, at 353 K*

Comparison of the spectra shows that by increasing the glyoxylic/glucosamine molar feed in the reaction, the degree of substitution also increases. In particular, by increasing the molar ratio of glyoxylic acid:glucosamine from 1:1 to 2:1 to 3:1 and to 4:1 the degree of substitution increases from **44%** to **58%** to **63%** and **66%**.

In addition, the effect of the reaction time on the DS was examined. **Figure 3.8** shows the ^{1}H NMR spectra of N-1:1 and N1-1:1 derivatives, prepared using the same molar ratio of GA/glucosamine (1:1), and reaction time 1.5 h and 24 h, respectively. From the ^{1}H NMR spectra we can observe a small change in the degree of substitution from **31%** to **40%,** with the increase of the reaction time.

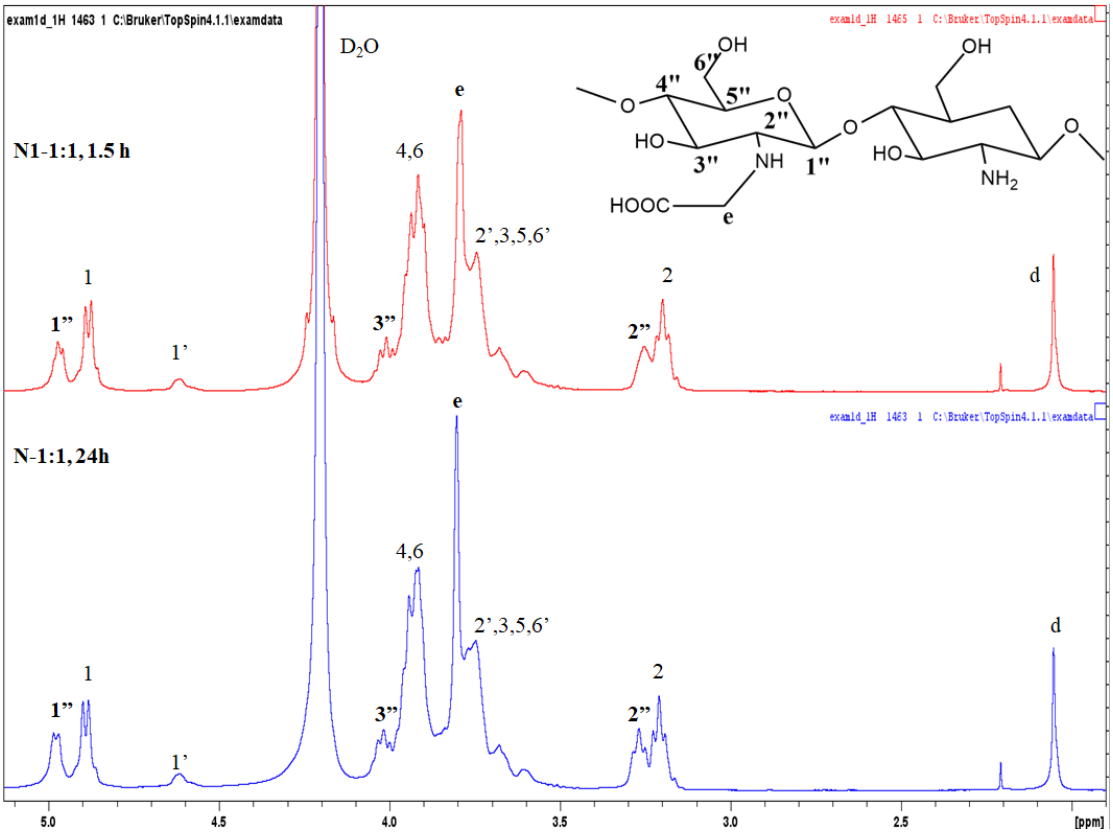

Fig.3.8. *^{1}H-NMR spectrum of N-Carboxymethyl chitosan derivatives, prepared at different reaction times, at 353K*

Finally, the effect of the addition of GA in the reaction, on the DS of chitosan was investigated. **Figure 3.9** shows the ^{1}H NMR spectra of N-3:1 and N3-3:1, where GA was added in one portion and three portions, within 3h, respectively. The DS of N-3:1

was found **63%** and for the N3-3:1 it was found **64%,** indicating that the mode of GA addition to the reaction does not affect the DS of chitosan.

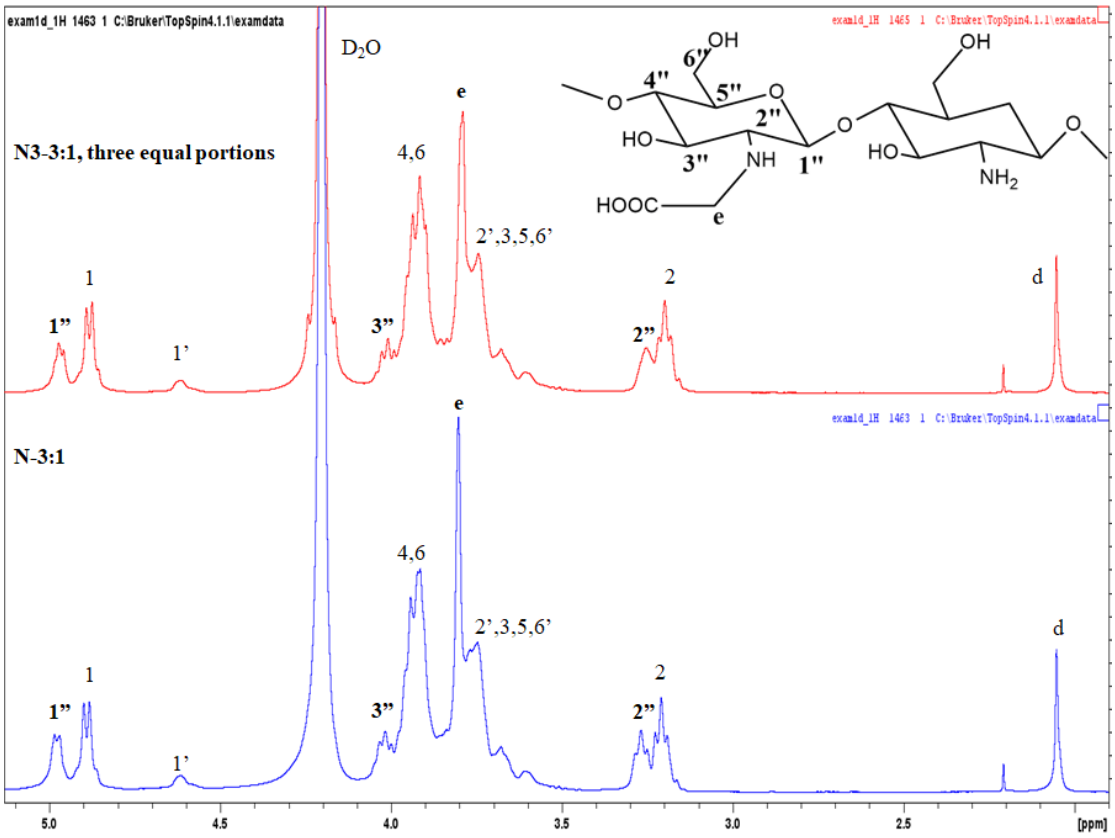

Fig.3.9. *^{1}H NMR spectra of N-Carboxymethyl chitosan derivatives, prepared at different modes GA addition, at 353 K*

Moreover, the chemical structure of NCMCs was studied by ^{13}C NMR spectroscopy. **Figure 3.10** shows the ^{13}C NMR spectrum of chitosan and of N-3:1 CMC at 301 K (28 °C). The ^{13}C NMR spectrum of N-3:1 presents four new peaks the **N-CH$_2$COOH**, **C2", C3", C1"** and **N-COOH**. The resonance at **51** ppm (**N-CH$_2$COOH**) is the signal of **CH$_2$** carbon arising from the GA grafted onto chitosan, the resonance signal at **64.5** ppm (**C2"**) is referred to the **2-carbon** of the modified structural unit, the resonance signal at **72.4** ppm (**C3"**) is assigned to the **3-carbon** of the modified structural unit, the resonance signal at **99.8** ppm (**C1"**) corresponds to the **1-carbon** of the modified structural unit and the resonance at **173** ppm (**N-COOH**) is the signal of the N-substituted carboxymethyl group. The absence of an additional peak at higher

ppm assigned to the carbon atom of carboxylic acid groups grafted onto the hydroxyl moieties of CMC, verified that only the N-substituted product was formed.

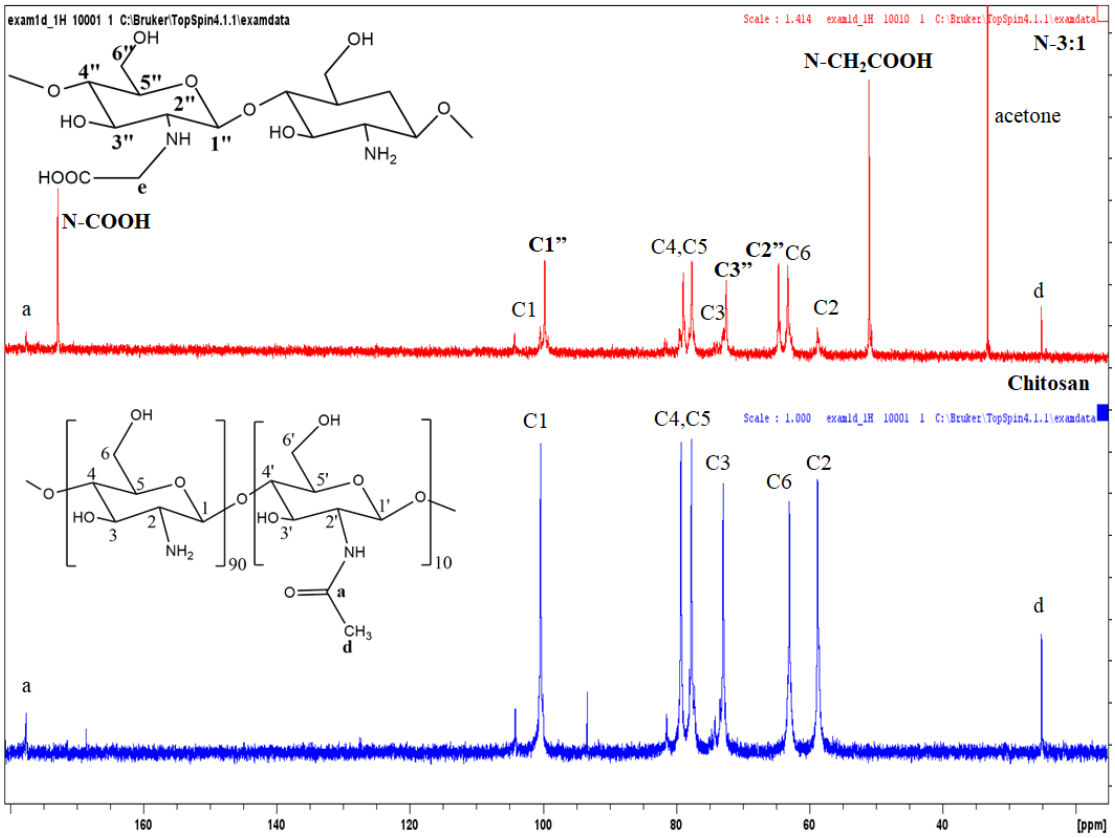

Fig.3.10. *^{13}C NMR spectra of chitosan and N-3:1 at 301 K*

Figure 3.11 shows the ^{13}C NMR spectra of chitosan and the different NCMCs derivatives at 301 K (28 °C). From these spectra we observed that as the DS increases the intensity of the **N-CH$_2$COOH**, **C2", C3", C1"** and **N-COOH** peaks also increase, while the intensity of the **C1**, **C2, C3** peaks, of the deacetylated unit of chitosan, decrease.

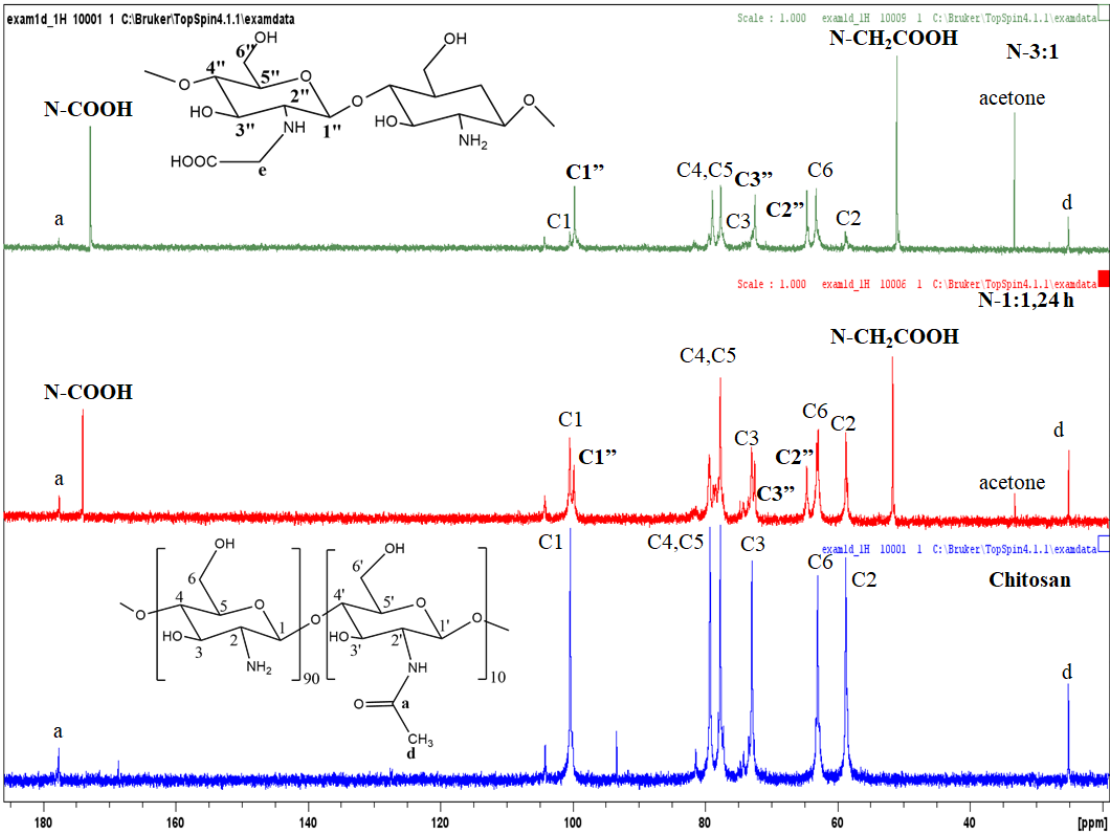

Fig.3.11. *^{13}C NMR spectra of chitosan and N-CMCs at 301 K*

Finally, HSQC NMR spectroscopy was employed for the characterization of N-CMC samples. **Figure 3.12** shows the HSQC NMR spectra of **N-1:1** at 301 K (28 ℃). The HSQC NMR spectra confirm the correlation between the proton peaks and carbons peaks. In particular, the ^{1}H-^{13}C correlation for **H2"/C2"** is observed at 3.3/65 ppm, that for **e** appeared at 3.8 ppm/ 51.5 ppm. In addition, the correlation **H3"/C3"** and for **H1"/C1"** are observed at 4 ppm/ 73 ppm and the 5 ppm/ 100 ppm.

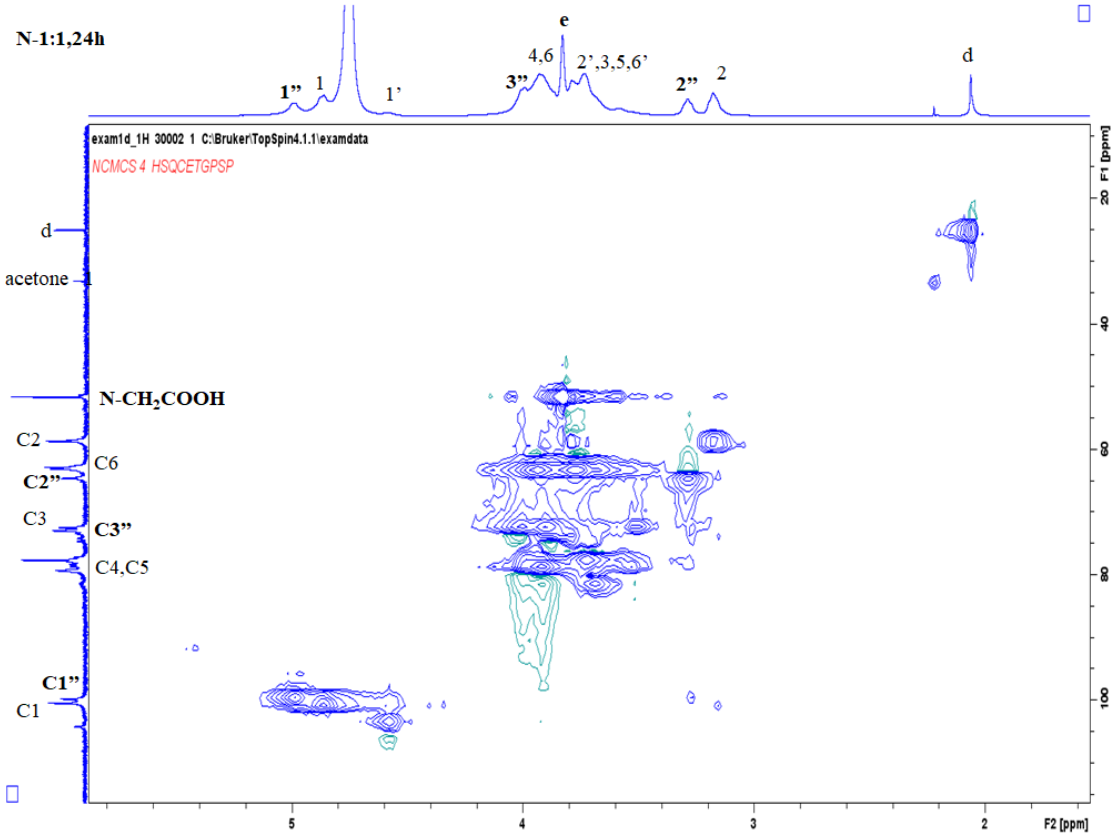

Fig.3.12. *HSQC NMR spectrum of N-1:1, 24h, in D_2O at 301 K*

Moreover, the structure and the chemical composition of the N-CMCs was studied by FTIR spectroscopy. **Figure 3.13** shows the FTIR spectra of chitosan and of N-3:1. The characteristic peaks of chitosan appear at 3455 cm^{-1}(**O-H stretching**), 2923-2867 cm^{-1}(**C-H stretching**), 1645 cm^{-1} (**C=O stretching**), 1598-1600 cm^{-1}(**N-H bending**), 1154 cm^{-1}(**bridge-O stretching**) and 1030 cm^{-1}(**C-O stretching**). By comparing the infrared spectra of chitosan with those of carboxymethyl chitosan, additional peaks are easily identified.[36] For the N-3:1 sample, the spectrum shows a new peak assigned to the C=O vibration of carboxylic acid moieties (**–COOH)** at 1741-1737 cm^{-1}. Moreover, the spectra of CMC show the bands at 1620 cm^{-1} and 1375 cm^{-1} corresponding to the **Asymmetric** and **symmetric** axial deformations of COO^- **carboxy** group (which overlaps with N-H bend), respectively [8,29]. The broader band centered at 3444 cm^{-1} indicates the hydrophilic character of the product.[37,38]

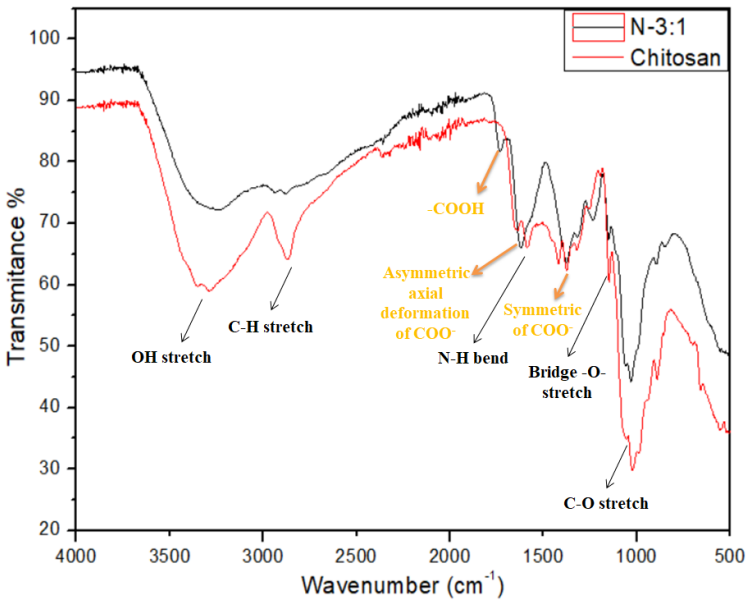

Fig.3.13. *FT-IR spectra of chitosan and N-3:1*

Figure 3.14 shows the FTIR spectra of chitosan and N-CMCs. An important observation is that when –COOH becomes ionized to its sodium salt –COONa, its absorption peak is shifted from 1730 cm^{-1} to 1598 cm^{-1}. This can be clearly observed for the N-1:1 sample (Figure 3.14).[25]

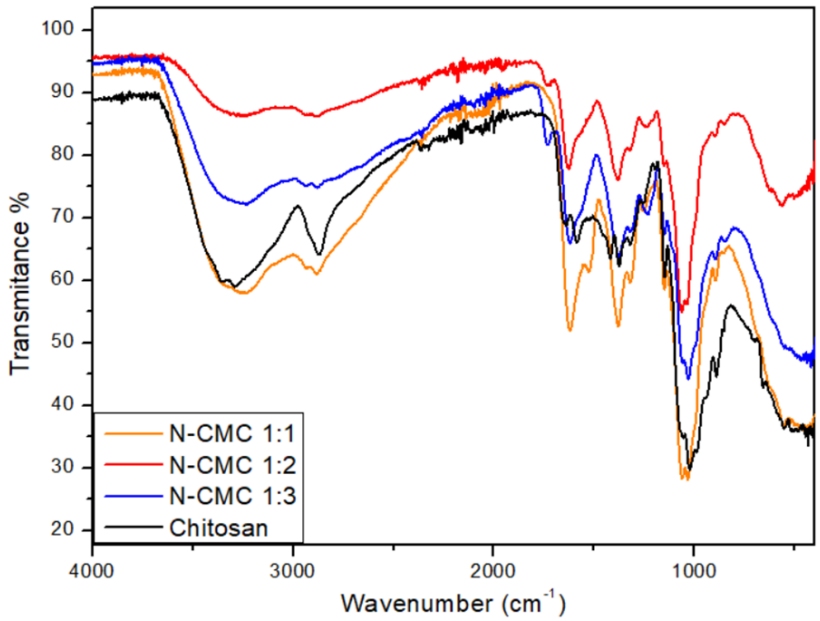

Fig.3.14. *FTIR spectra of chitosan and the N-CMCs*

Finally, the thermal stability of N-carboxymethyl chitosan derivatives was examined by TGA. **Figure 3.15** shows the TGA curves of chitosan and of the N-CMCs. It is clear from the TGA curves that carboxymethylation reduces the thermal stability of chitosan. Chitosan starts to degrade at around 300℃, while the degradation temperature for the N-CMCs is at ~200℃. In particular, for the N-1:1 and N-2:1 samples, with 40% and 58% DS, respectively, the degradation temperature is around 233 ℃, while, for the N-3:1 and N-4:1 samples with 64% and 66% DS, respectively the degradation temperature decreases to 200℃. To conclude, as the degree of substitution increases, the decomposition temperature decreases. [39]

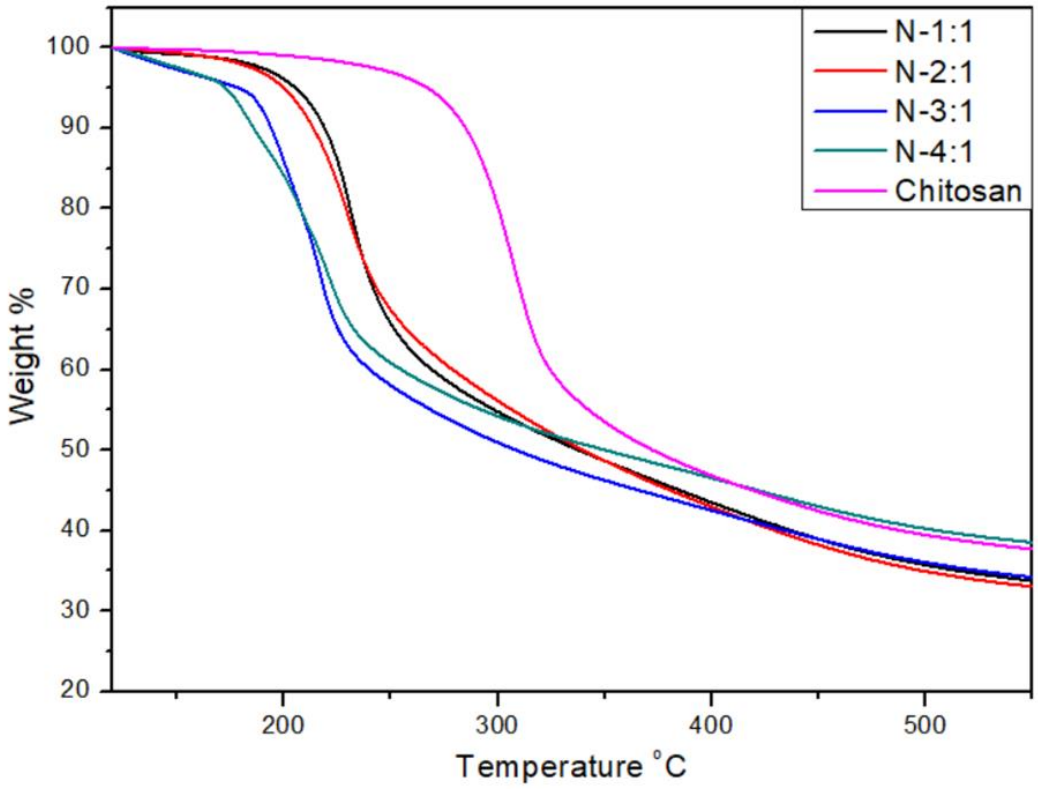

Fig.3.15. *TGAs curve of chitosan and the NCMCs*

3.4 Characterization of N,O-carboxymethyl chitosan derivatives

The successful synthesis of the N,O-carboxymethyl chitosan derivatives was verified by ^{1}H NMR spectroscopy. **Figure 3.16** shows the ^{1}H NMR spectra of chitosan and of the **N,O-1-33%** carboxymethyl chitosan derivative, prepared using **8:1** molar ratio of monochloroacetic acid/chitosan and 33% w/v NaOH. The ^{1}H NMR

spectra were obtained at 325 K, because at higher temperature, the **g** and **f** peaks overlap with the solvent peak (D_2O).

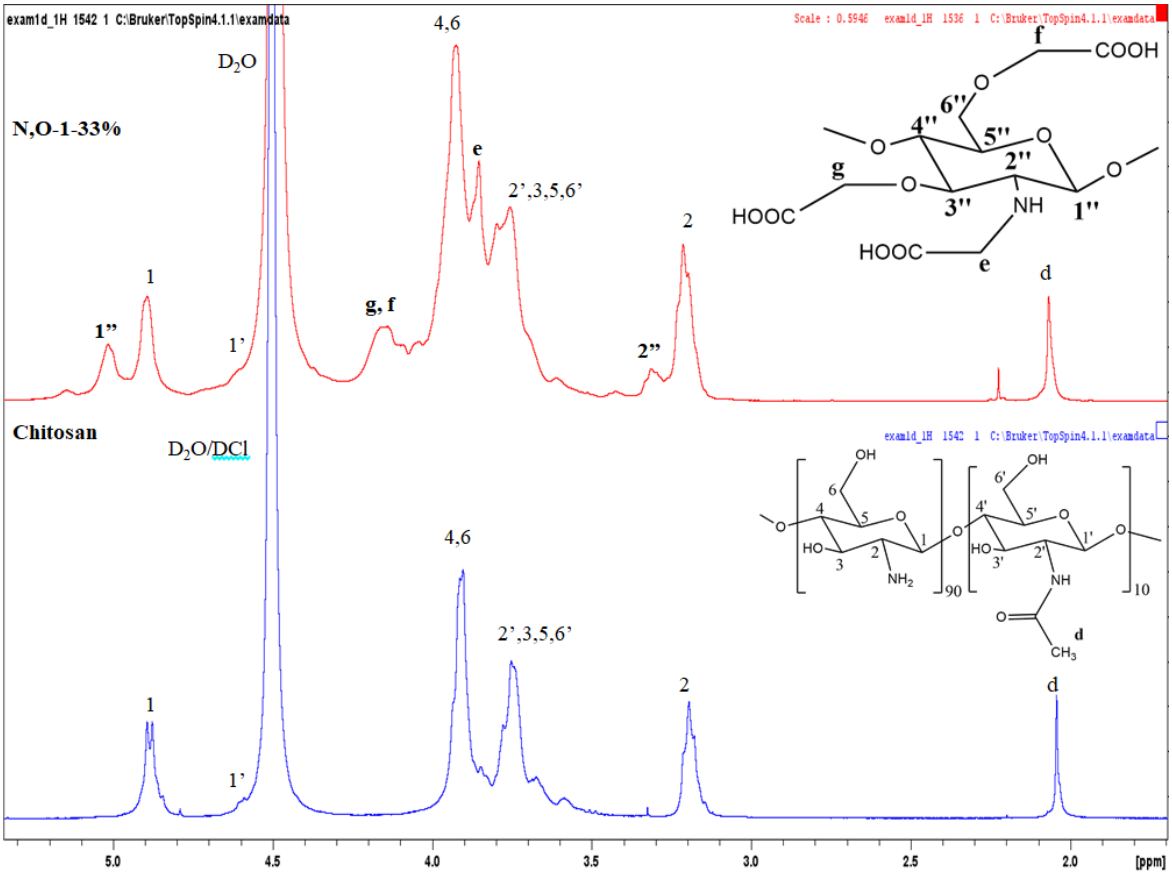

Fig.3.16. *^{1}H NMR spectrum of chitosan and of N,O-1-33% at 325 K*

The ^{1}H NMR spectrum of N,O-CMC, N,O-1-33% showed six new peaks at **3.3**, **3.4**, **3.8**, between **4-4.3** ppm, **5** and **5.15** ppm compared to those of chitosan . The **2"** peak at **3.3** ppm is assigned to the H-2D proton of the modified structural unit, the peak at **3.4** ppm is assigned to the **2-modified carbon** when it's disubstituted **(N-$(CH_2)_2$COOH)**. The peak **e** at **3.8** ppm corresponds to the 2 protons of **N-CH_2-COOH** and the peaks **g, f** in the between **4-4.3** ppm are assigned to the **2** protons of **3-O-CH_2COOH** and **6-O-CH_2COOH,** respectively. Finally, the peak at **5** ppm is the signal of the protons of the 1-modified carbon when it is disubstituted **(N-$(CH_2)_2$COOH)** and the peak **1"** at **5.15** ppm is assigned to the **H-1D** proton of the modified structural unit.

The degree of substitution on the amine groups was determined by rationing the integrals of the peaks **1"** to **d** while by rationing the integral of the peaks **g and f** to **d** the degree of substitution on the hydroxyl groups was calculated. When this approach could not be used to determine the DS, the total DS was obtained from the integrals of the peaks between **3.5** and **4.3** ppm. The contribution of the chitosan protons, which is constant, was subtracted and from the known N-substitution, the O-substitution was obtained. The degree of substitution of all the N,O-carboxymethyl chitosan derivatives prepared is presented at **Table 3.3**, and the O-selectivity is presented in **Table 3.4**. In addition, the degree of substitution of the amine groups (DS-N) refers to the degree of substitution per 100 deacetylated structural units, while the degree of substitution of the hydroxyl groups (DS-O) is defined per 100 modified units of chitosan.

Table 3.3 Degree of substitution of N,O-carboxymethyl chitosan derivatives

Samples	MCA:chitosan Molar Ratio	W/I (v/v)	NaOH w/v %	T(°C)	Time (h)	pH	DS
N,O-10%	8:1	1:4	**10**	60	3	8-8.5	**30%**
N,O-12,5%	8:1	1:4	**12.5**	20	4	12	**48%**
N,O-1-33%	8:1	1:1	**33**	20	4	14	**112%**
N,O-2-33%	8:1	1:1	**33**	60	4	14	**125%**
N,O-1-50%	8:1	1:1	**50**	20	4	14	**138%**
N,O-2-50% 1h swelling	4:1	1:1	**50**	20	4	14	**73%**
N,O-3-50% 24h swelling	4:1	1:1	**50**	20	4	14	**74%**

Table 3.4 Degree of substitution and O-selectivity of N,O-CMCs				
Samples	DS	DS-N	DS-O	O-selectivity
N,O-10%	**30%**	**11%**	**19%**	**63%**
N,O-12.5%	**48%**	**12%**	**36%**	**75%**
N,O-1-33%	**112%**	**38%**	**74%**	**66%**
N,O-2-33%	**125%**	**36%**	**89%**	**71%**
N,O-1-50%	**138%**	**28%**	**110%**	**80%**
N,O-2-50%-1h swelling	**73%**	**20%**	**53%**	**73%**
N,O-3-50%-24h swelling	**74%**	**19%**	**55%**	**74%**

Figure 3.17 shows the ^{1}H NMR spectra of the N,O-carboxymethyl chitosan derivatives prepared at different NaOH concentrations using the same molar ratio of chloroacetic acid/chitosan repeat units (8:1), in comparison to that of chitosan at 325 K.

The DS that are above 100% mean that more than one reactive group may have been substituted in a structural unit. The data presented in **Table 3.2** show that as the concentration of NaOH increases, so does the degree of substitution. By increasing the NaOH concentration from **10** w/v% to **33** w/v% and to **50** w/v% the DS increased from **30**% to **112**% to **138**%, while the O-selectivity also increased from **63**% to **66**% to **80**%. However, under all the reaction conditions examined in this study it was not possible to achieve the selective derivatization at the hydroxyl groups only to form O-CMC. In the carboxymethylation process, a **50** w/v% NaOH solution seems to provide the best results. The rigid crystalline structure of chitosan proved difficult to break at lower NaOH concentrations to ensure that chloroacetic acid penetration into the interlocking polymer chains, and resulted in a reduced DS.[8] According to the literature, a high alkali concentration above 60% stimulated a side reaction between NaOH and chloroacetic acid, lowering the available chloroacetic for the reaction.[40] It is worth mentioning that chitosan at strongly alkaline pH values may deacetylate. By increasing the NaOH concentration from **12.5** w/v% to **33** w/v% and to **50** w/v% an increase on the degree of deacetylation was observed from **91**% to **94**% and **96**%.

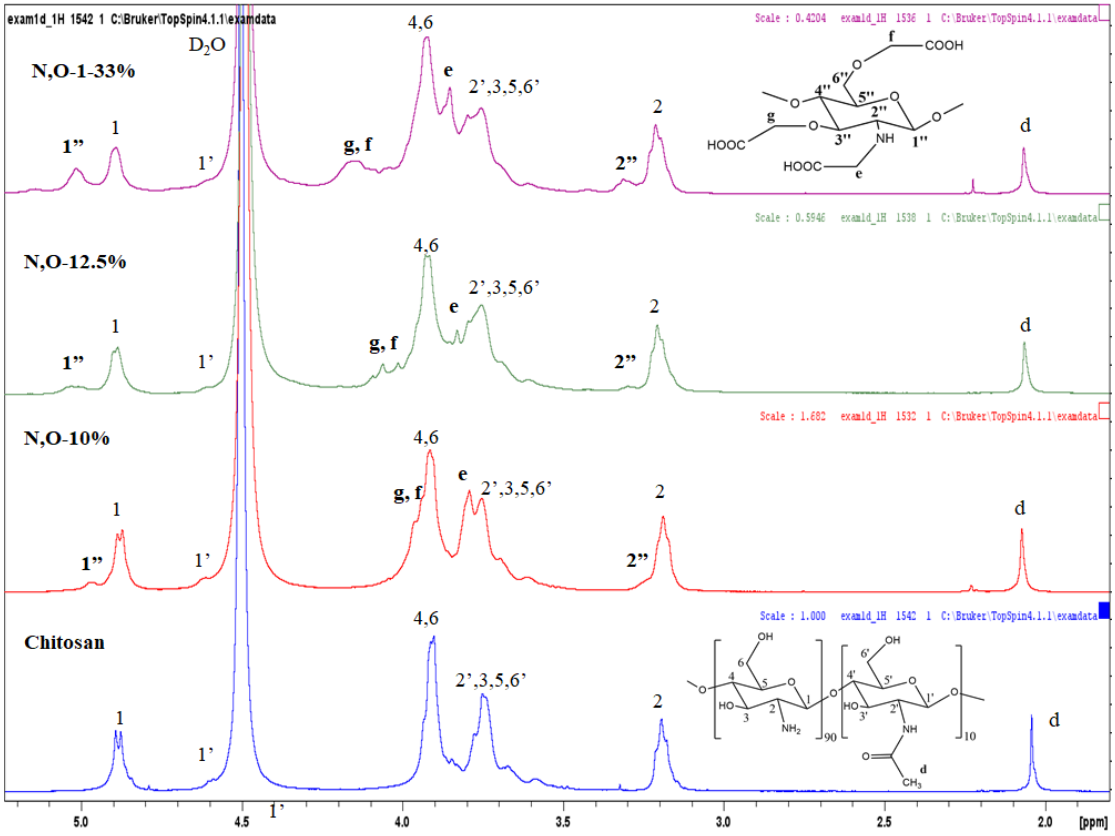

Fig.3.17. *^{1}H NMR spectra of chitosan and the N,O-Carboxymethyl chitosan derivatives prepared at different NaOH concentrations and the same chloroacetic acid/chitosan sugar residues mole ratio at 325 K*

Furthermore, the water/isopropanol volume fraction is an important factor affecting the carboxymethylation reaction. When chitosan is reacted in isopropanol alone, the yield is low, but when water is used as the only solvent, the yield is even lower. The reason is the swelling of the carboxymethyl chitosan formed in water, which coats the insoluble chitosan and prohibits the penetration of monochloroacetic acid to the polymer mass, thus reducing the reaction yield. For this, in all the reaction of chitosan with mocnochloroacetic acid 1:1 and 1:4 (v:v) mixture of water/isopropanol, was employed. The reaction yield decreases and the polymer insolubility increases at higher pH as the water/isopropanol ratio increases.[25] Another important finding is that the increase of the monochloroacetic acid/chitosan sugar residues from **4:1** to **8:1** leads to a higher DS as expected.

Finally, the effect of the reaction temperature on the DS was examined. **Figure 3.18** shows the ^{1}H NMR spectra of the N,O-carboxymethyl chitosan derivatives prepared at different reaction temperature. The DS of **N,O-1-33%-20℃** and of **N,O-1-33%-60℃** was calculated to be **112%** and **125%** respectively indicating that the temperature does not significantly affect the DS**.** Similarly, the O-selectivity slightly increased from **66** % to **71**% as the reaction temperature increased from 20℃ to 60 ℃.

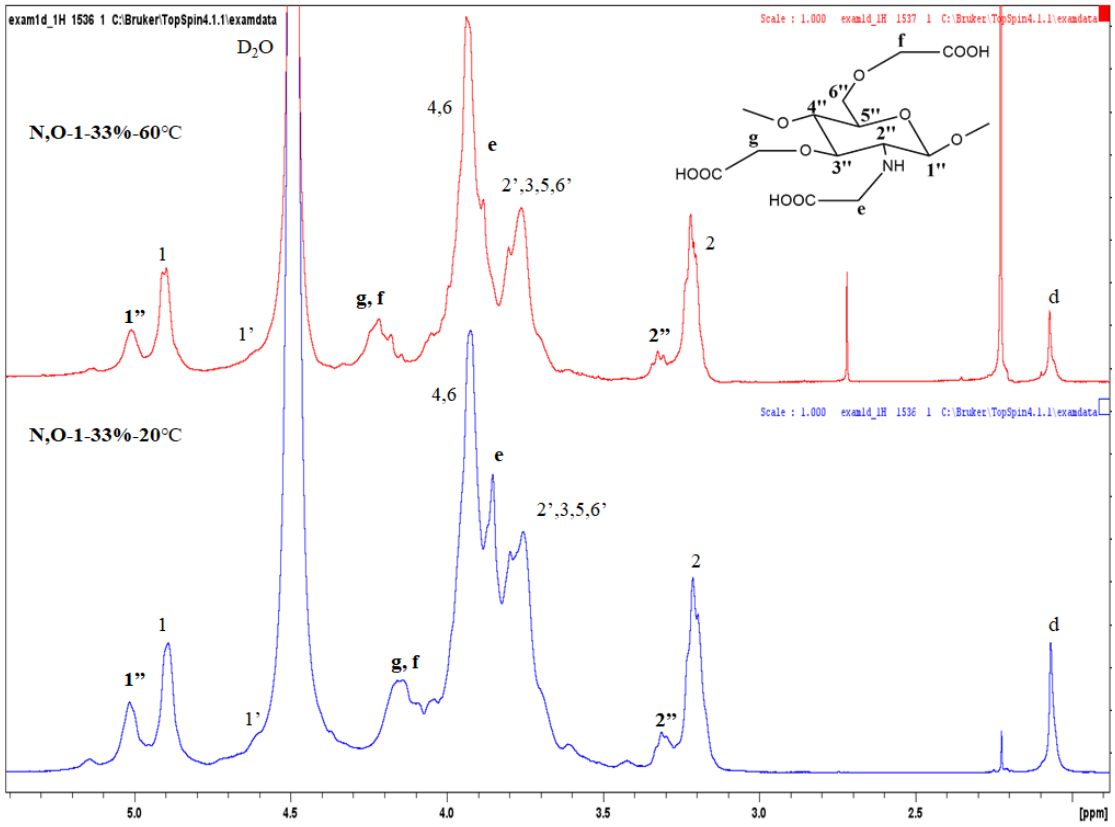

Fig.3.18. *^{1}H NMR spectra of N,O-1-33%-20℃ and N,O-1-33%-60℃ at 325 K*

Finally, the effect of the time allowed for the chitosan to swell in the basic solutions prior to the addition of MCA was examined. **Figure 3.19** shows the ^{1}H NMR spectra of the N,O-carboxymethyl chitosan derivatives, for which chitosan was allowed to swell for 1 h and 24 h. The conclusion that can be drawn is that for the same molar ratio of chloroacetic acid/chitosan sugar residues the swelling does not affect the O-selectivity and the DS which was found **73**% and **74**% for the N,O-2-50%-1h swelling and N,O-3-50%-24h swelling, respectively.

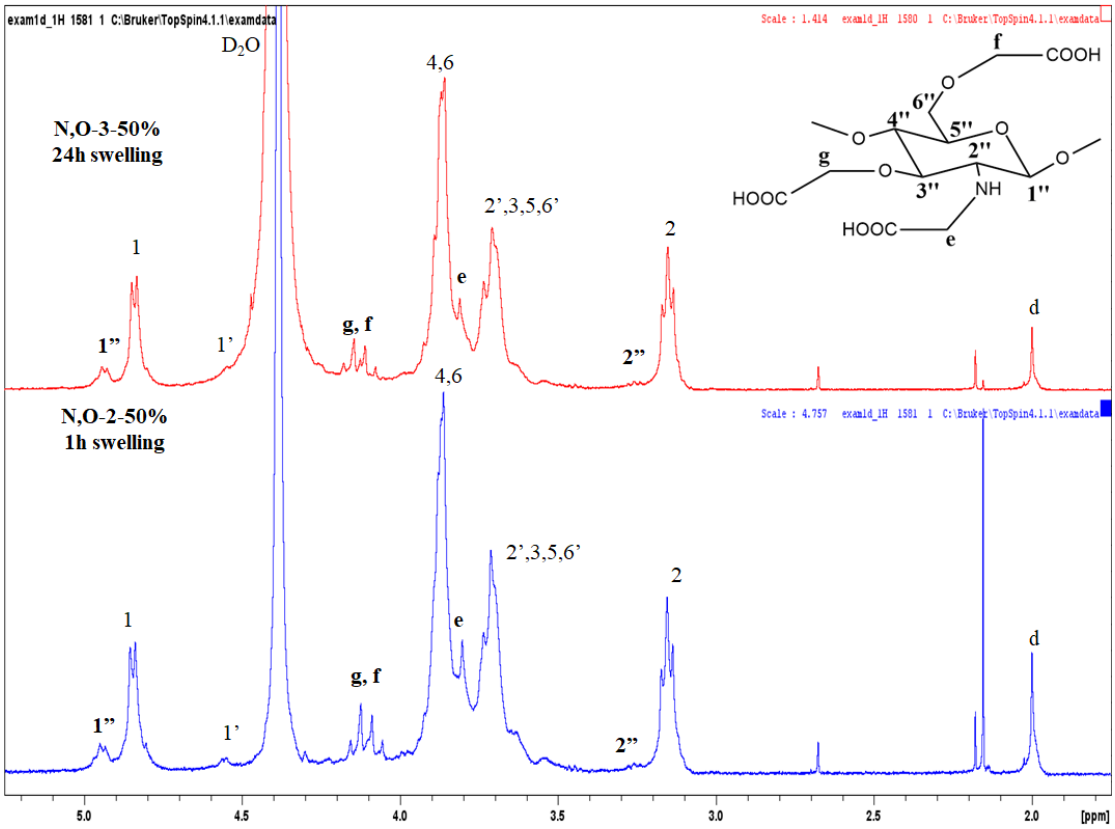

Fig.3.19. *^{1}H NMR spectra of N,O-3-50%-24h swelling and N,O-2-50%-1h swelling at 325 K*

Moreover, the chemical structure of the N,O-CMCs was studied by ^{13}C NMR spectroscopy. **Figure 3.20** shows the ^{13}C NMR spectra of chitosan and the N,O-CMCs at 301 K (28°C). The ^{13}C NMR spectra of the N,O-CMCs present eight new peaks at **51.8**, **64.6, 72.3, 72.5, 76.4, 99.8, 173** and **180.3** ppm. The resonance at **51.8** ppm (**N-CH_2COOH**) is the signal of the **CH_2** carbon atom of the modified structural unit, the resonance signal at **64.6** ppm (**C2"**) is referred to the **2-carbon** of the modified structural unit, the resonance signal at **72.3** ppm (**g**) is referred to the signal of **CH_2** carbon of the **3-O-CH_2COOH** group, the resonance signal at **72.5** ppm (**f**) is referred to the signal of **CH_2** carbon of the **6-O-CH_2COOH** group, the resonance signal at **99.8** ppm is referred to the disubstituted carbon **N-$(CH_2)_2$COOH** of the modified structural unit, the resonance at **173** ppm (**N-COOH**) is the signal of the N-substituted carboxymethyl group and the resonance at **180.3** ppm (**O-COOH**) is the signal of the O-substituted carboxymethyl group. From the above the substitution at both the amine and the hydroxyl groups of chitosan is evident.

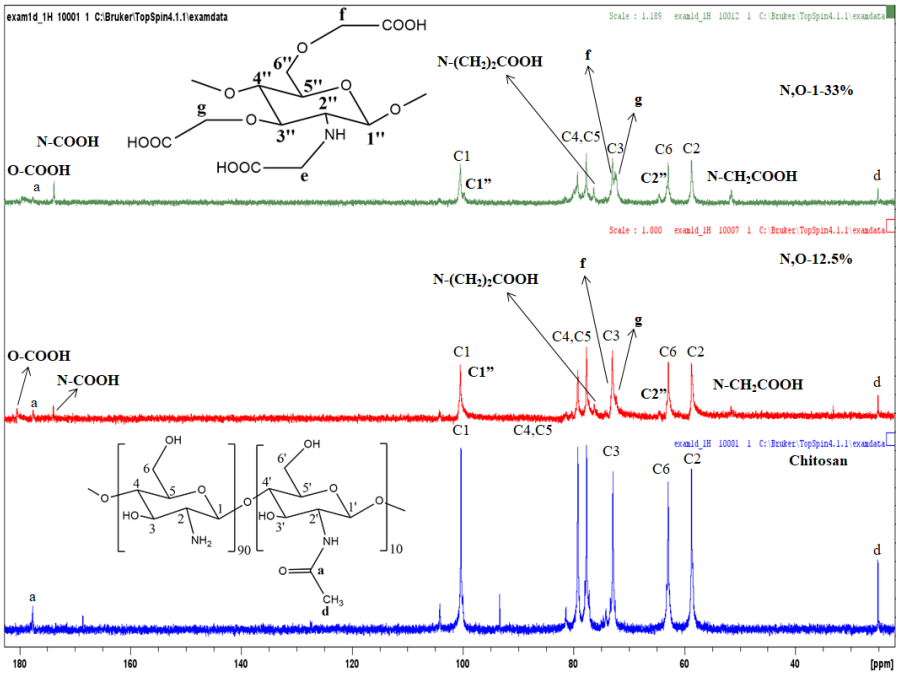

Fig.3.20. *^{13}C NMR of chitosan and the N,O-CMCs at 301 K*

Finally, HSQC NMR spectroscopy was employed for the characterization of N,O-CMCs samples. **Figure 3.21** shows the HSQC NMR spectra of **N,O-1-33%** at 301 K (28 °C). HSQC NMR spectra confirm the correspondence between protons peaks and carbons peaks.

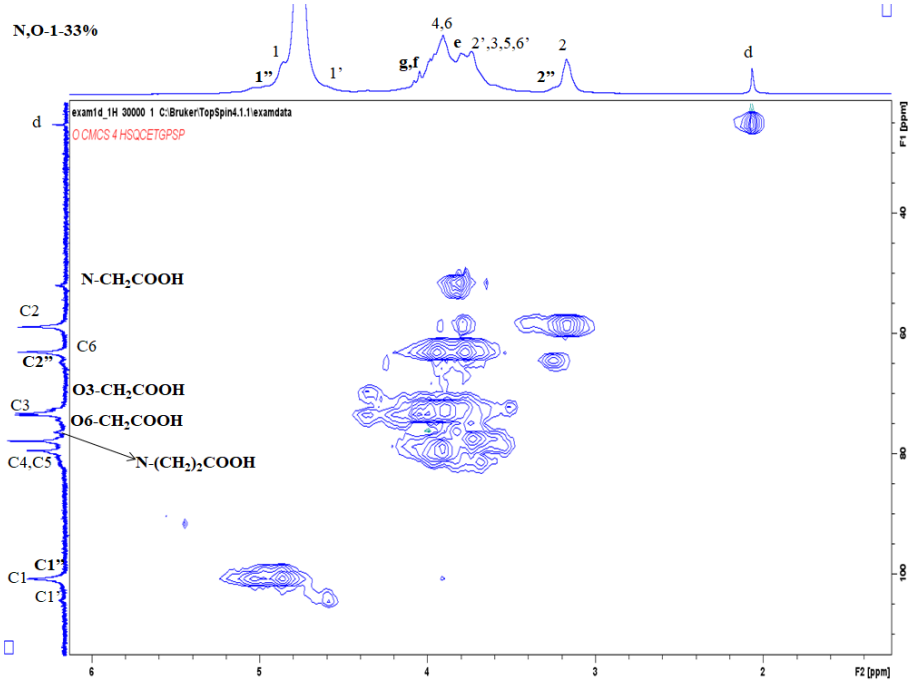

Fig.3.21. *HSQC NMR spectrum of N,O-1-33% in D_2O at 301 K*

Moreover, the structure and the chemical composition of the N,O-CMCs was studied with FTIR spectroscopy. **Figure 3.22** shows the FTIR spectra of chitosan and the N,O-derivatives. The characteristic peaks of chitosan appear at 3455 cm^{-1}(**O-H stretch**), 2923-2867 cm^{-1}(**C-H stretch**), 1645 cm^{-1} (**C=O stretching**), 1598-1600 cm^{-1}(**N-H bend**), 1154 cm^{-1}(**bridge-O stretch**) and 1030 cm^{-1}(**C-O stretch**). By comparing the infrared spectrum of chitosan with that of carboxymethyl chitosan, the following structural changes are easily identified.[36] For the N,O-CMCs sample , the spectrum shows a new peak at 1741-1737 cm^{-1}assigned to the C=O vibration of carboxylic acid moieties (**–COOH)**. Furthermore, in the spectra of the N,O-CMC samples the bands at 1620 cm^{-1} and 1375 cm^{-1}, corresponding to the **Asymmetric** and **symmetric** axial deformations of COO^- **carboxy** group (which overlaps with the N-H bending vibration), respectively are intense[8,29]. The appearance of a broader band, centered at 3444 cm^{-1}, as compared to the precursor chitosan spectrum, indicates the hydrophilic character of the product. Finally the **C-O** stretching band at 1030 cm^{-1} shifted to 1070 cm^{-1} which corresponds to **C-O-C** stretching, verifying carboxymethylation occurred at the C6 position[37,38].

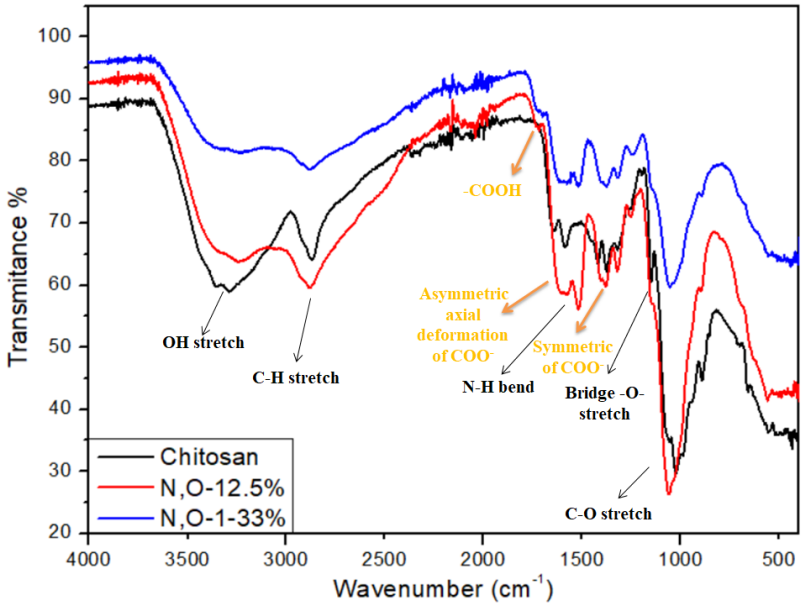

Fig.3.22. *FTIR spectrum of chitosan and the N,O-CMCs*

Finally, the thermal properties N,O-Carboxymethyl chitosan derivatives were investigated. **Figure 3.23** shows the TGA curves of chitosan and the N,O-CMCs. The thermal stability of chitosan reduces upon carboxymethylation as discussed above. More specifically, chitosan degrades at around 300 ℃, while the degradation temperature for the N,O-CMCs in at ~ 215 ℃.[39]

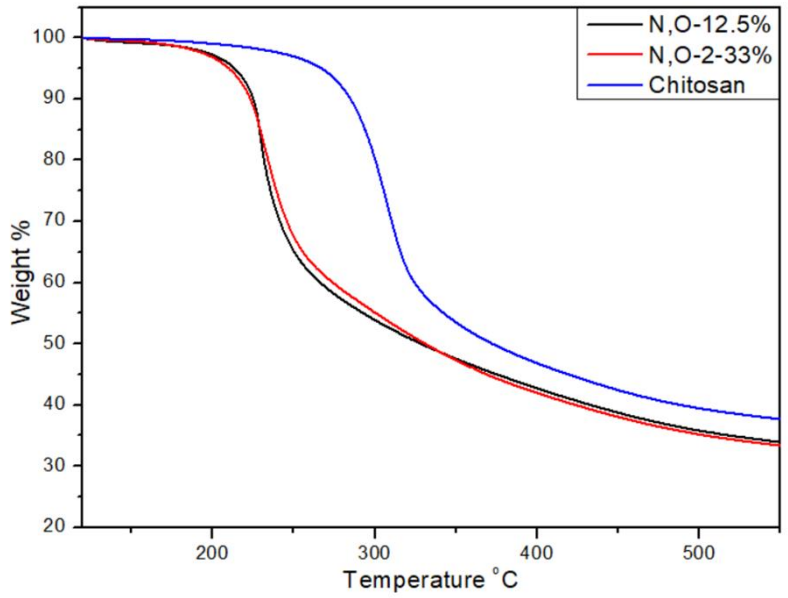

Fig.3.23. *TGA curves of chitosan and of the N,O-CMCs*

3.5 Comparison of carboxymethylated chitosan derivatives

^{1}H NMR spectroscopy was used to compare two different derivatives, **N-4:1** and **N,O-3-50%,** with the same degree of substitution. **Figure 3.24** shows the ^{1}H NMR spectra of **chitosan**, **N-4:1** and **N,O-3-50%** with DS of **73%** and **74%,** respectively at 325 K. The main difference between the two samples is the appearance of the **g,f** peaks for the **N,O-3-50%** which indicates the O-carboxymethylation. Furthermore, the intensity of the peak **e, 1" and 2"** peaks appears to decrease for the N,O derivative, which verifies the lower modification of the amino groups.

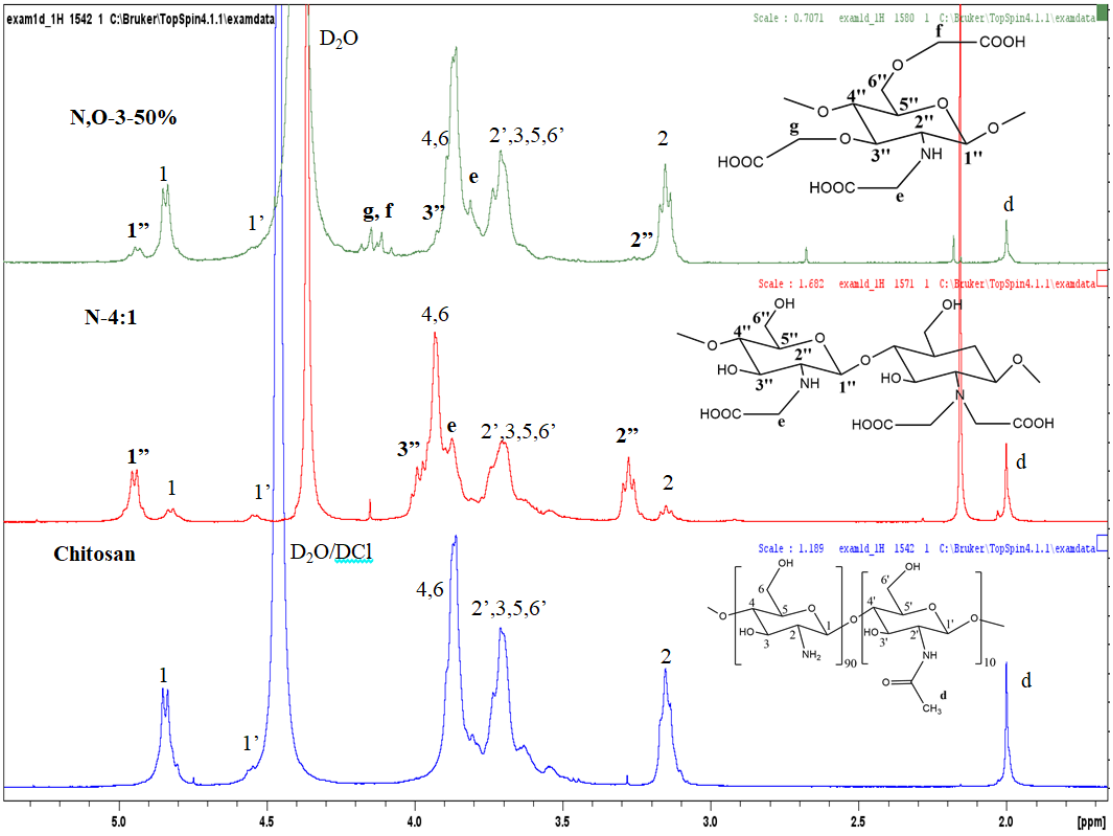

Fig.3.24. *^{1}H NMR spectra of chitosan and N-4:1 and of N,O-3-50%*

In addition, ^{13}C-NMR spectroscopy was used to compare the two different derivatives. **Figure 3.25** shows the ^{1}H-NMR spectra of **chitosan**, **N-3:1** and **N,O-12.5%** at 301K. The first big difference between the two samples is the appearance of the peaks **N-(CH$_2$)$_2$COOH, O-COOH and g,f** for the **N,O-12.5%** that indicates the disubstitution and the O-carboxymethylation respectively. Furthermore, the intensity of the peak**s C1" and C2"** appears to increase to the N-derivative, which verifies higher modification in the amino groups.

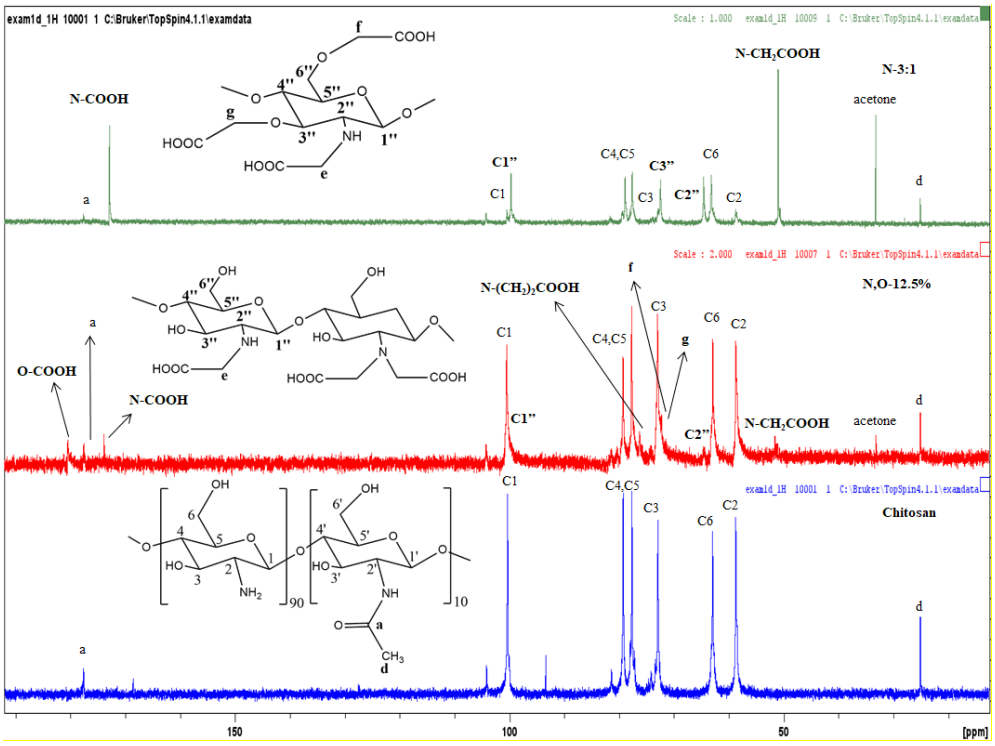

Fig.3.25. *^{13}C-NMR spectrum of chitosan, N-3:1 and N,O-12.5% at 301 K*

Moreover, the structure of N-4:1 and of N,O-3-50% was studied by FT-IR spectroscopy. **Figure 3.26** shows the FT-IR spectra of chitosan and of the N-4:1 and of N,O-3-50%. The peaks **–COOH**, and **-symmetric and asymmetric axial deformation of COO$^-$** appear in both materials. The main difference between them is that at the **N-4:1** spectrum the peak of the symmetric axial deformation of COO$^-$ overlaps the N-H bending because of the high degree of substitution at the amine groups which is not observed for the N,O derivative. In addition, for the N-derivative the **symmetric and asymmetric axial deformation of COO$^-$** peaks are very sharp. This indicates the higher degree of substitution of the amine groups.

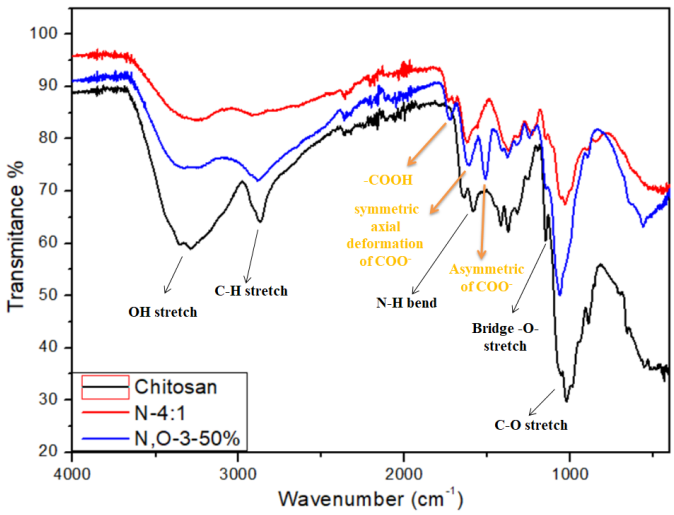

Fig.3.26. *FT-IR spectrum of chitosan, N-4:1 and N,O-3-50%*

Finally, the TGA technique was used to compare the thermal stability of two derivatives with similar DS. **Figure 3.27** shows the TGA curves of chitosan, **N:1-1** and **N,O-12.5%** with DS of **40%** and **48%** respectively. As seen from the TGA curves, CMC samples of approximately the same DS exhibit similar thermal properties regardless of where the substitution is performed (N:1-1 substitution takes place only at the amine groups, while N,O-12.5% has O-selectivity 75%).

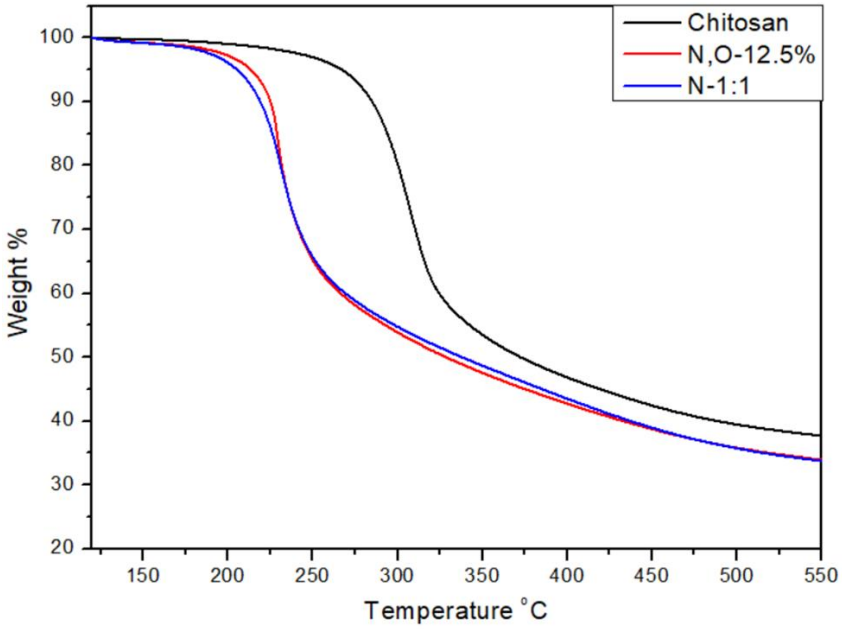

Fig.3.27. *TGA curve of chitosan, N:1-1 and N,O-12.5%*

Chapter 4

Conclusions and future perspectives

Despite the variety of studies to synthesize site specific CMCs, there is not yet a very precise method allowing to produce these specifically modified chitosans, which could be capitalized to produce even more potent biomaterials. Therefore, in this thesis, a series of carboxylated chitosan derivatives modified either at its amino or both amino and hydroxyl side-groups, with different degrees of modification, were prepared.

Carboxymethyl chitosan derivatives were successfully synthesized and were fully characterized by ^{1}H NMR, ^{13}C NMR and HSQC NMR spectroscopies. The structure and the chemical composition of each sample were also studied by FTIR spectroscopy, while their thermal stability was determined with TGA.

More specifically, for the preparation of the N-derivatives reductive alkylation was employed. In this reaction the NH_2 groups of chitosan react with the aldehyde groups of glyoxylic acid, followed by hydrogenation with $NaBH_4$. In this case, N-CMCs were successfully prepared with degree of substitution ranging from 31% to 66%, by varying the glyoxylic/glucosamine molar ratio from 1:1 to 4:1.

On the other hand, for the N,O-derivatives direct alkylation was used. This method utilizes monochloroacetic acid to prepare N-carboxyalkyl and O-carboxyalkyl chitosan derivatives under different reaction conditions. More specifically a series of N,O-CMCs samples were prepared, in which the molar ratio of monochloroacetic acid/chitosan sugar residues was varied from 4:1 to 8:1, the volume ratio of water/isopropanol from 1:1 to 1:4 v/v and the w/v NaOH concentration at 10%, 12.5%, 33% and 50%. The aim of this reaction was to substitute only the hydroxyl groups, but due to the high activity of the amino groups it is inevitable to prepare only O-derivatives. By using the above approach N,O-derivatives with degrees of substitution ranging from 30% to 138% were obtained while the O-selectivity was varied between 66 % and 80 %.

As future work, to prepare O-derivatives, the amino groups of chitosan could be protected with a protecting group, namely Fmoc, and then deprotected after the

carboxymethylation reaction. These materials will be employed to investigate the effect of the site-specific functionalization of the chitosan side-groups on its biological properties in tissue engineering applications. For this, the materials could be used to prepare scaffolds for tissue engineering applications by electrospinning. Electrospinning (Electrostatic fiber spinning) is a modern and efficient method which uses an electric field to produce fine fibers with diameters in the nanometer range. These fibers in the form of mats are very attractive as 3D cell scaffolds in tissue engineering.

Chapter 5

Characterization Techniques

5.1 NMR Spectroscopy

Nuclear magnetic resonance spectroscopy (NMR) is a powerful analytical technique used to determine the chemical structure of compounds and biomolecules in solution. The identification and structural elucidation of organic, metal-organic, and biological compounds have been the most important chemical applications of proton NMR spectroscopy. An NMR spectrum, seldom suffices by itself for the identification of an organic compound. However, in conjunction with mass, IR, and UV spectra, as well as elemental analysis, NMR is a powerful and indispensable tool for the characterization of pure compounds.[41]

The NMR spectrometer uses a magnetic field and a special detector to assess the changes (**Fig.5.1.**). The external magnetic field causes electrically charged nuclei to move from a lower energy level (E1) to a higher energy level (E2) and the difference between E2 and E1 is symbolized as ΔE which is dependent on the power of the magnetic field and the size of the nuclear field moment. The electromagnetic radiation rhythm attains the NMR signal with a frequency (v) causing the nuclei to move to a higher energy level (E1/E2). When this electromagnetic radiation is stopped, it causes the nuclei to relax and accomplish thermal equilibrium. This release of energy from the nuclei is recorded in the form of spectra on the computer, and these spectra are exclusive for every nucleus and are equivalent to the energy levels between the two states (E2/E1)(**Fig.5.2.**). [42,43]

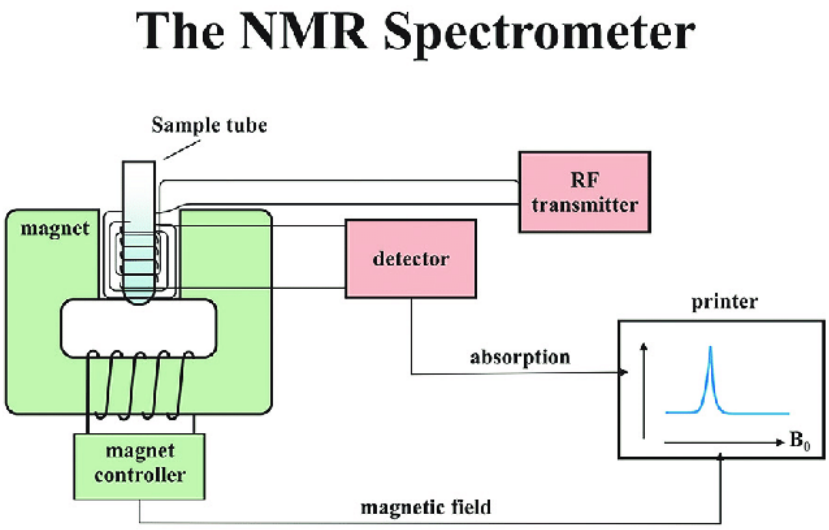

Fig.5.1. *Schematic presentation of a typical nuclear magnetic resonance spectrometer* [43]

The basic principle of this method is presented below. The sample tube is placed in a magnetic field and the NMR signal is produced by the excitation of the sample with radiowaves into a nuclear magnetic resonance, which is detected with sensitive radio receivers. The signal gives the necessary information about the nuclei's surroundings. The exact field strength (in ppm) of a nucleus comes into resonance relative to a reference standard, usually the signal of the deuterated solvent used. The nuclei are shielded from the external magnetic field by electron clouds, allowing them to absorb more energy (lower ppm), whereas nearby functional groups 'desield' the nuclei, allowing them to absorb less energy (higher ppm). Nuclei that are chemically and magnetically equal resonant at the same energy and produce a single signal or pattern. Protons interact and split each other's resonances into multiple peaks following the n+1 rule. The area under the NMR peak is proportional to the number of nuclei that give rise to that resonance thus by integration, the protons of that resonance can be calculated.

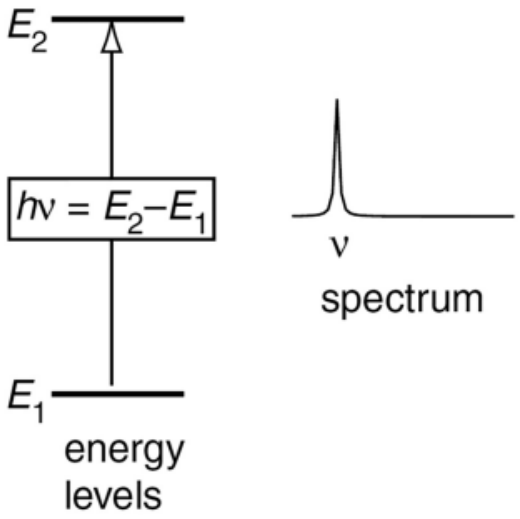

Fig.5.2. *A line in the spectrum is associated with the transition between two energy levels* [42]

5.2 FTIR Spectroscopy

Fourier transform infrared spectroscopy is a powerful analytical technique and it is the most common form of infrared spectroscopy. FTIR it the most preferred method of infrared spectroscopy for several reasons. First, it is a non-destructive method. Second it is faster and third it is much more precise and sensitive. These advantages of FTIR stem from the use of an interferometer, which acts as an infrared 'source' and allows for faster processing, as well as the Fourier transform. The Fourier transform is a mathematical function that deconstructs waves and returns the wave's frequency as a function of time.

To absorb IR radiation, a molecule must undergo a net change in dipole moment as it vibrates or rotates. The alternating electric field of the radiation can only interact with the molecule under these conditions and produces changes in the amplitude of one of its movements. For example, the charge distribution around a molecule such as hydrogen chloride is not symmetric because the chlorine has a higher electron density than the hydrogen. Thus, hydrogen chloride has a significant dipole moment and is said to be polar. The dipole moment is determined by the magnitude of the charge difference and the distance between the two centers of charge. As a hydrogen chloride molecule vibrates, a regular fluctuation in its dipole moment occurs, and a field is established that can interact with the electric field associated with radiation. If the

frequency of the radiation exactly matches the molecule's natural vibrational frequency, the radiation is absorbed, resulting in a change in the amplitude of the molecular vibration. Similarly, the rotation of asymmetric molecules around their centers of mass results in periodic dipole moment fluctuations that allow interaction with the radiation field. No net change in dipole moment occurs during the vibration or rotation of homonuclear species such as O_2, N_2, or Cl_2. As a result, such compounds cannot absorb IR radiation. With the exception of a few compounds of this type, all other molecular species absorb IR radiation.[41]

The relative positions of atoms in a molecule fluctuate continuously because of a multitude of different types of vibrations and rotations about the bonds in the molecule. There are two basic categories of vibrations: stretching and bending. These are shown schematically in **Figure 5.3**.[41]

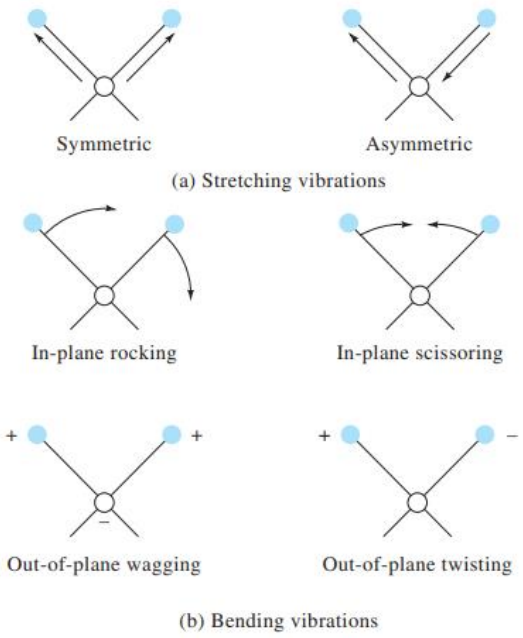

Fig.5.3. *Main types of vibration. +indicates motion from the page toward the reader and – indicates motion away from the reader*[41]

The basic principle of operation of the FTIR spectrometer is shown in **Figure 5.4.** Briefly, radiation of all frequencies from the IR source is reflected into the interferometer, where it is modulated by the moving mirror on the left. The modulated

radiation is then reflected from the two mirrors on the right through the sample in the compartment at the bottom. After passing through the sample, the radiation falls on the transducer. A data-acquisition system attached to the transducer records the signal and stores it in the memory of a computer as an interferogram.[41]

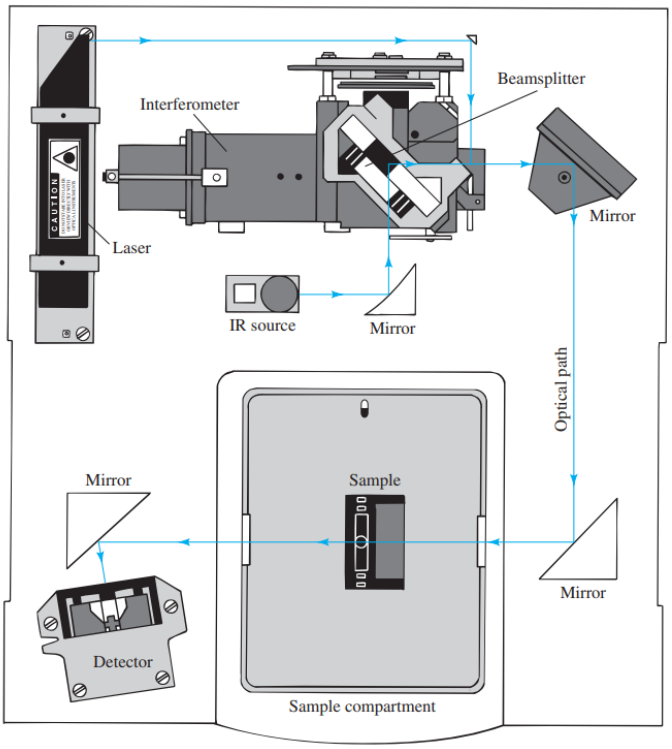

***Fig.5.4**. Diagram of a basic FTIR spectrometer.*[41]

5.3 Thermogravimetric analysis (TGA)

TGA (thermogravimetric analysis) is an experimental technique that measures the weight or, more precisely, the mass of a sample as a function of sample temperature or time. The sample is normally heated at a constant heating rate (so-called dynamic measurement) or kept at a constant temperature (isothermal measurement), but non-linear temperature programs, such as those used in sample controlled TGA (so-called SCTA) experiments. The type of information required for the sample will determine which temperature program is used. Furthermore, the atmosphere utilized in the TGA experiment is critical and can be reactive, oxidizing or inert. The results of a TGA measurement are usually displayed as a TGA curve in which mass or per cent mass is plotted against temperature and/or time.[44]

Commercial instruments for TGA consist of a sensitive microbalance, called a thermobalance, a furnace, a pure-gas system for providing an inert, or sometimes reactive, atmosphere and a computer system for instrument control, data acquisition and data processing. A pure-gas switching system is a common option for applications in which the purge gas must be changed during an experiment.[41]

Different effects might cause a sample to lose or gain mass, resulting in TGA curve steps. The following are some of them[41]:

- Evaporation of volatile compounds; drying; adsorption and desorption of gases, moisture and other ingredients; loss of water (**Figure 5.5**)
- Oxidation of metals and oxidative decomposition of organic substances in air or oxygen

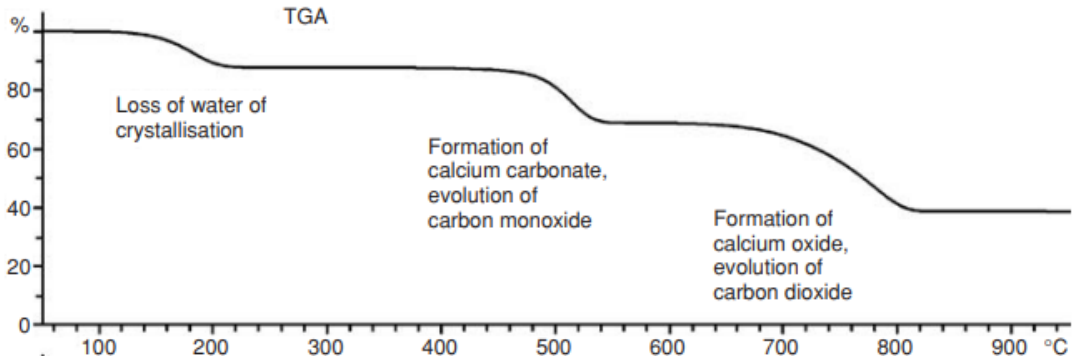

Fig.5.5. *Stepwise decomposition of calcium oxalate monohydrate: sample mass 19 mg, heating rate 30 K/min, under nitrogen*[44]

Thermograms provide information regarding the decomposition mechanisms for various polymers. Moreover, the decomposition patterns are unique to each type of polymer and can be utilized to identify it in some cases.

References

[1] J. Park, R.S. Lakes, Biomaterials, An Introduction, Third Edit, 2007.

[2] R.C. Thomson, M.C. Wake, M.J. Yaszemski, A.G. Mikos, Biodegradable polymer scaffolds to regenerate organs, Adv. Polym. Sci. 122 (1995) 218–274. https://doi.org/10.1007/3540587888_18.

[3] J.S. Temenoff, A.G. Mikos, Biomaterials: The intersection of Biology and Materials Science, 2008.

[4] A.G. Gristina, P.T. Naylor, Q.N. Myrvik, Biomaterial-Centered Infections: Microbial Adhesion versus Tissue Integration, Pathog. Wound Biomater. Infect. 7 (1990) 193–216. https://doi.org/10.1007/978-1-4471-3454-1_25.

[5] J.E. Mark, Physical Properties of Polymers Handbook, Second Edi, Springer, 2007. https://doi.org/10.1007/BF01840027.

[6] S.M. Ahsan, M. Thomas, K.K. Reddy, S.G. Sooraparaju, A. Asthana, I. Bhatnagar, Chitosan as biomaterial in drug delivery and tissue engineering, Int. J. Biol. Macromol. 110 (2018) 97–109. https://doi.org/10.1016/j.ijbiomac.2017.08.140.

[7] K. Sakurai, Structure of Chitin and Chitosan, Sen'i Gakkaishi. 46 (1990) P-553-P-557. https://doi.org/10.2115/fiber.46.12_P553.

[8] V.K. Mourya, N.N. Inamdar, A. Tiwari, Carboxymethyl chitosan and its applications, Adv. Mater. Lett. 1 (2010) 11–33. https://doi.org/10.5185/amlett.2010.3108.

[9] L.T. Ng, S. Swami, IPNs based on chitosan with NVP and NVP/HEMA synthesised through photoinitiator-free photopolymerisation technique for biomedical applications, Carbohydr. Polym. 60 (2005) 523–528. https://doi.org/10.1016/j.carbpol.2005.03.009.

[10] J. Berger, M. Reist, J.M. Mayer, O. Felt, R. Gurny, Structure and interactions in chitosan hydrogels formed by complexation or aggregation for biomedical applications, Eur. J. Pharm. Biopharm. 57 (2004) 35–52. https://doi.org/10.1016/S0939-6411(03)00160-7.

[11] J. Berger, M. Reist, J.M. Mayer, O. Felt, N.A. Peppas, R. Gurny, Structure and interactions in covalently and ionically crosslinked chitosan hydrogels for biomedical applications, Eur. J. Pharm. Biopharm. 57 (2004) 19–34. https://doi.org/10.1016/S0939-6411(03)00161-9.

[12] K.A. Northcott, I. Snape, P.J. Scales, G.W. Stevens, Dewatering behaviour of water

treatment sludges associated with contaminated site remediation in Antarctica, Chem. Eng. Sci. 60 (2005) 6835–6843. https://doi.org/10.1016/j.ces.2005.05.049.

[13] G. Crini, Recent developments in polysaccharide-based materials used as adsorbents in wastewater treatment, Prog. Polym. Sci. 30 (2005) 38–70. https://doi.org/10.1016/j.progpolymsci.2004.11.002.

[14] M. Rinaudo, Chitin and chitosan: Properties and applications, Prog. Polym. Sci. 31 (2006) 603–632. https://doi.org/10.1016/j.progpolymsci.2006.06.001.

[15] Y.C. Chung, H.L. Wang, Y.M. Chen, S.L. Li, Effect of abiotic factors on the antibacterial activity of chitosan against waterborne pathogens, Bioresour. Technol. 88 (2003) 179–184. https://doi.org/10.1016/S0960-8524(03)00002-6.

[16] F. Ham-Pichavant, G. Sèbe, P. Pardon, V. Coma, Fat resistance properties of chitosan-based paper packaging for food applications, Carbohydr. Polym. 61 (2005) 259–265. https://doi.org/10.1016/j.carbpol.2005.01.020.

[17] A. Jimtaisong, N. Saewan, Utilization of carboxymethyl chitosan in cosmetics, Int. J. Cosmet. Sci. 36 (2014) 12–21. https://doi.org/10.1111/ics.12102.

[18] L. Upadhyaya, J. Singh, V. Agarwal, R.P. Tewari, Biomedical applications of carboxymethyl chitosans, Carbohydr. Polym. 91 (2013) 452–466. https://doi.org/10.1016/j.carbpol.2012.07.076.

[19] Z. Shariatinia, Carboxymethyl chitosan: Properties and biomedical applications, Int. J. Biol. Macromol. 120 (2018) 1406–1419. https://doi.org/10.1016/j.ijbiomac.2018.09.131.

[20] M. Mattioli-Belmonte, A. Gigante, R.A.A. Muzzarelli, R. Politano, A. De Benedittis, N. Specchia, A. Buffa, G. Biagini, F. Greco, N,N-dicarboxymethyl chitosan as delivery agent for bone morphogenetic protein in the repair of articular cartilage, Med. Biol. Eng. Comput. 37 (1999) 130–134. https://doi.org/10.1007/BF02513279.

[21] Z. Shi, K.G. Neoh, E.T. Kang, K.P. Chye, W. Wang, Surface Functionalization of Titanium with Carboxymethyl Chitosan and Immobilized Bone Morphogenetic Protein-2 for Enhanced Osseointegration, Biomacromolecules. 10 (2009) 1603–1611. https://doi.org/10.1021/bm900203w.

[22] D. Mishra, B. Bhunia, I. Banerjee, P. Datta, S. Dhara, T.K. Maiti, Enzymatically crosslinked carboxymethyl-chitosan/gelatin/nano- hydroxyapatite injectable gels for in

situ bone tissue engineering application, Mater. Sci. Eng. C. 31 (2011) 1295–1304. https://doi.org/10.1016/j.msec.2011.04.007.

[23] R.A.A. Muzzarelli, P. Ilari, M. Petrarulo, Solubility and structure of N-carboxymethylchitosan, Int. J. Biol. Macromol. 16 (1994) 177–180. https://doi.org/10.1016/0141-8130(94)90048-5.

[24] X.F. Liu, Y.L. Guan, D.Z. Yang, Z. Li, K. De Yao, Antibacterial action of chitosan and carboxymethylated chitosan, J. Appl. Polym. Sci. 79 (2001) 1324–1335. https://doi.org/10.1002/1097-4628(20010214)79:7<1324::AID-APP210>3.0.CO;2-L.

[25] X.G. Chen, H.J. Park, Chemical characteristics of O-carboxymethyl chitosans related to the preparation conditions, Carbohydr. Polym. 53 (2003) 355–359. https://doi.org/10.1016/S0144-8617(03)00051-1.

[26] S.C. Chen, Y.C. Wu, F.L. Mi, Y.H. Lin, L.C. Yu, H.W. Sung, A novel pH-sensitive hydrogel composed of N,O-carboxymethyl chitosan and alginate cross-linked by genipin for protein drug delivery, J. Control. Release. 96 (2004) 285–300. https://doi.org/10.1016/j.jconrel.2004.02.002.

[27] H.C. Ge, D.K. Luo, Preparation of carboxymethyl chitosan in aqueous solution under microwave irradiation, Carbohydr. Res. 340 (2005) 1351–1356. https://doi.org/10.1016/j.carres.2005.02.025.

[28] N. Kubota, Y. Eguchi, Facile preparation of water-soluble N-acetylated chitosan and molecular weight dependence of its water-solubility, Polym. J. 29 (1997) 123–127. https://doi.org/10.1295/polymj.29.123.

[29] D. De Britto, S.P. Campana-Filho, A kinetic study on the thermal degradation of N,N,N-trimethylchitosan, Polym. Degrad. Stab. 84 (2004) 353–361. https://doi.org/10.1016/j.polymdegradstab.2004.02.005.

[30] F.R. de Abreu, S.P. Campana-Filho, Preparation and characterization of carboxymethylchitosan, Polímeros. 15 (2005) 79–83. https://doi.org/10.1590/s0104-14282005000200004.

[31] Y. Shigemasa, H. Matsuura, H. Sashiwa, H. Saimoto, Evaluation of different absorbance ratios from infrared spectroscopy for analyzing the degree of deacetylation in chitin, Int. J. Biol. Macromol. 18 (1996) 237–242. https://doi.org/10.1016/0141-8130(95)01079-3.

[32] J. Brugnerotto, J. Lizardi, F.M. Goycoolea, W. Argüelles-Monal, J. Desbrières, M. Rinaudo, An infrared investigation in relation with chitin and chitosan characterization, Polymer (Guildf). 42 (2001) 3569–3580. https://doi.org/10.1016/S0032-3861(00)00713-8.

[33] I. Corazzari, R. Nisticò, F. Turci, M.G. Faga, F. Franzoso, S. Tabasso, G. Magnacca, Advanced physico-chemical characterization of chitosan by means of TGA coupled on-line with FTIR and GCMS: Thermal degradation and water adsorption capacity, Polym. Degrad. Stab. 112 (2015) 1–9. https://doi.org/10.1016/j.polymdegradstab.2014.12.006.

[34] H. Moussout, H. Ahlafi, M. Aazza, M. Bourakhouadar, Kinetics and mechanism of the thermal degradation of biopolymers chitin and chitosan using thermogravimetric analysis, Polym. Degrad. Stab. 130 (2016) 1–9. https://doi.org/10.1016/j.polymdegradstab.2016.05.016.

[35] M. Ziegler-Borowska, D. Chełminiak, H. Kaczmarek, Thermal stability of magnetic nanoparticles coated by blends of modified chitosan and poly(quaternary ammonium) salt, J. Therm. Anal. Calorim. 119 (2015) 499–506. https://doi.org/10.1007/s10973-014-4122-7.

[36] S.S. Vaghani, M.M. Patel, C.S. Satish, K.M. Patel, N.P. Jivani, Synthesis and characterization of carboxymethyl chitosan hydrogel: Application as site specific delivery for lercanidipine hydrochloride, Bull. Mater. Sci. 35 (2012) 1133–1142. https://doi.org/10.1007/s12034-012-0413-4.

[37] F.R. de Abreu, S.P. Campana-Filho, Characteristics and properties of carboxymethylchitosan, Carbohydr. Polym. 75 (2009) 214–221. https://doi.org/10.1016/j.carbpol.2008.06.009.

[38] Z. Zhao, Z. Wang, N. Ye, S. Wang, A novel N, O-carboxymethyl amphoteric chitosan/poly(ethersulfone) composite MF membrane and its charged characteristics, Desalination. 144 (2002) 35–39. https://doi.org/10.1016/S0011-9164(02)00285-0.

[39] P. Kumar, E. Faujdar, R.K. Singh, S. Paul, A. Kukrety, V.K. Chhibber, S.S. Ray, High CO2 absorption of O-carboxymethylchitosan synthesised from chitosan, Environ. Chem. Lett. 16 (2018) 1025–1031. https://doi.org/10.1007/s10311-018-0713-z.

[40] R.A.A. Muzzarelli, F. Tanfani, M. Emanuelli, S. Mariotti, N-(carboxymethylidene)chitosans and N-(carboxymethyl)chitosans: Novel chelating

polyampholytes obtained from chitosan glyoxylate, Carbohydr. Res. 107 (1982) 199–214. https://doi.org/10.1016/S0008-6215(00)80539-X.

[41] D.A. Skoog, J.F. Holler, S.R. Crouch, Principles of Instrumental Analysis, Seventh, 2018.

[42] J. Keeler, Understanding NMR spectroscopy, Choice Rev. Online. 43 (2002) 43-5896-43–5896. https://doi.org/10.5860/choice.43-5896.

[43] K. Zia, T. Siddiqui, S. Ali, I. Farooq, M.S. Zafar, Z. Khurshid, Nuclear Magnetic Resonance Spectroscopy for Medical and Dental Applications: A Comprehensive Review, Eur. J. Dent. 13 (2019) 124–128. https://doi.org/10.1055/s-0039-1688654.

[44] P. Gabbott, Principles and Applications of Thermal Analysis, 2008. https://doi.org/10.1002/9780470697702.